

KeyB2: Selecting Key Blocks is Also Important for Long Document Ranking with Large Language Models

MINGHAN LI, Soochow University, China

ERIC GAUSSIER, Université Grenoble Alpes, France

JUNTAO LI, Soochow University, China

GUODONG ZHOU, Soochow University, China

The emergence of large language models (LLMs) such as Llama has significantly advanced neural information retrieval (IR). However, applying LLMs to long document reranking remains computationally expensive and may be ineffective. Moreover, the internal behavior of LLMs during document relevance judgment is still underexplored. In this paper, we begin with an in-depth analysis of decoder-only LLM attention patterns and find that several attention heads consistently align with relevance signals, yet this alignment deteriorates as irrelevant content increases. Motivated by this observation, we revisit and extend the block selection paradigm, introducing KeyB2, a scalable reranking framework that combines block pre-selection with powerful decoder-only LLMs. KeyB2 generalizes the selection stage to support BM25, cross-encoder, and bi-encoder, and adapts LLM to compute fine-grained relevance scores. We further introduce a new bi-encoder strategy that performs strongly and efficiently. Extensive experiments on TREC DL 2019/2023 document task, Robust04, and MLDR-zh demonstrate that KeyB2 outperforms baselines including RankLLaMA, RankLLaMA-MaxP/AvgP, and KeyB, achieving new state-of-the-art (SOTA) results on TREC DL 2019 document reranking task. In addition, KeyB2 reduces reranking latency compared with RankLLaMA by over 83% and memory usage by over 74%, positioning it as a practical and effective solution for long document ranking with LLMs.

CCS Concepts: • **Information systems** → **Information retrieval; Retrieval models and ranking; Language models; Document representation.**

Additional Key Words and Phrases: Long-document neural information retrieval, large language models

1 Introduction

The rapid development of LLMs such as GPT and Llama has transformed diverse natural language processing (NLP) tasks, including IR, text generation, and comprehension. These models have demonstrated remarkable capabilities in capturing deep semantic relationships within text, leading to significant advancements in IR systems. Cross-encoder models, such as RankLLaMA [34], have been particularly effective at evaluating the relevance of queries and passages by encoding entire input sequences jointly. Despite these advancements, processing long documents with LLMs remains challenging, primarily due to the quadratic complexity of self-attention mechanisms, leading to high computational and memory demands. Furthermore, there remains room for improvement in the effectiveness of directly using LLMs.

In practical applications, such as legal document retrieval, enterprise search, and academic research, efficiently handling long documents is essential, as relevant information can be spread across lengthy text. Techniques like block selection, which divides long documents into smaller segments and focuses on the most pertinent portions, have emerged as practical solutions to reduce computational demands. The KeyB approach [30] has demonstrated that selectively processing key blocks can enhance both retrieval efficiency and accuracy. However, as LLM architectures continue to evolve, revisiting block selection strategies is crucial to fully exploit the potential of these strategies in long document IR.

Moreover, the internal mechanisms of LLMs during the ranking process are still not fully understood, particularly how these models weigh and align relevant content between queries and documents. Understanding the

Authors' Contact Information: Minghan Li, mhli@suda.edu.cn, Soochow University, Suzhou, China; Eric Gaussier, Eric.Gaussier@univ-grenoble-alpes.fr, Université Grenoble Alpes, Grenoble, France; Juntao Li, ljt@suda.edu.cn, Soochow University, Suzhou, China; Guodong Zhou, gdzhou@suda.edu.cn, Soochow University, Suzhou, China.

role of attention mechanisms in relevance judgement remains a key challenge, and it is essential to investigate how specific attention heads contribute to aligning query terms with document content in the context of IR.

In this paper, we propose KeyB2, an enhanced block selection strategy designed to integrate seamlessly with LLMs like Llama, combining efficient block selection with the advanced semantic matching capabilities of modern models. Additionally, compared to KeyB models, we incorporate a bi-encoder-based block selection strategy, enhancing the balance between efficiency and semantic comprehension. The KeyB2 approach aims to address the computational challenges associated with long document processing while leveraging LLMs' contextual understanding to improve ranking performance. By selectively identifying and processing key blocks, KeyB2 reduces computational overhead and enhances retrieval effectiveness, making it well-suited for large-scale IR tasks.

To explore the potential of the KeyB2 approach, we investigate the following research questions:

RQ1 Interpretability. How do large-language-model rerankers allocate attention between query and document tokens during relevance estimation, and do the resulting patterns suggest that relevance cues are concentrated in a limited set of blocks?

RQ2 Ranking Effectiveness. Does pairing an LLM with an explicit block selector (KeyB2) improve long-document ranking effectiveness over the the KeyB approach and full-document LLM reranker (RankLLaMA)?

RQ3 Selector Design. Which block-selection strategy—lexical (BM25), neural bi-encoder, or neural cross-encoder—achieves the best balance between selection quality and computational overhead when integrated with an LLM backbone?

RQ4 Computational Efficiency. To what extent does block selection reduce inference latency and GPU memory compared with full-document LLM rerankers, and where do KeyB2 variants lie on the accuracy–efficiency Pareto frontier?

Our contributions are summarized as follows:

- We provide an in-depth attention analysis of LLM rerankers (RankLLaMA), opening the black box and showing that full-document LLMs struggle with attention dispersion in long-document retrieval tasks, especially in noisy contexts, motivating the need for explicit block selection.
- We propose KeyB2, a generalization of the KeyB framework that integrates block selection into LLM-based reranking. KeyB2 extends the original KeyB design by adopting stronger LLaMA2 and LLaMA3 backbones and supporting flexible block selectors (BM25, bi-encoder, cross-encoder).
- We conduct comprehensive experiments on four datasets (TREC DL19/23 document reranking, Robust04, MLDR-zh), covering in-domain, cross-domain, and bi-lingual scenarios. KeyB2 consistently outperforms prior baselines, including full-document RankLLaMA and previous KeyB models, achieving new SOTA on TREC 2019 DL document reranking task.
- We systematically analyze the computational efficiency of KeyB2, demonstrating that block selection allows substantial reductions in inference latency and GPU memory usage while maintaining or improving ranking accuracy.

The structure of this paper is as follows: Section 2 reviews related work in LLM-based information retrieval, including recent developments in reranking and block selection. Section 3 conducts a comprehensive attention-based analysis of RankLLaMA to investigate whether it internally captures relevance between queries and long documents, thereby addressing RQ1. Section 4 introduces the proposed KeyB2 approach, including its architecture and differences from prior KeyB methods. Section 5 and Section 6 present the experimental setup and results, analyzing retrieval effectiveness (RQ2), robustness under noisy conditions (RQ3), and computational efficiency (RQ4). Finally, Section 7 concludes the paper and outlines future directions.

2 Related Work

2.1 From Neural-IR Models to Pre-trained Language Models for Information Retrieval

Pre-trained language models (PLMs) have reshaped the field of IR. Initially, models such as the Deep Structured Semantic Model (DSSM) [60] laid the groundwork by employing fully connected networks for representations, mapping queries and documents into a shared semantic space through non-linear projections. Other studies in this area have aimed to leverage distributed representations through variations of DSSM or employed alternative representation functions [16, 36, 37, 47].

Early neural IR models like DRMM [12] outperformed traditional methods by utilizing interaction functions and term-level relevance networks. KNRM Xiong et al. [51] employs a translation matrix using word embeddings to represent word-level similarities. KNRM’s unique kernel-pooling technique extracts multi-level soft match features, and its learning-to-rank layer integrates these features into a final ranking score. This end-to-end trained model tunes word embeddings to generate desired soft matches, demonstrating the effectiveness of neural networks in capturing nuanced relationships between query terms and document content. Inspired by the human judgment process for document relevance, Pang et al. [38] introduce DeepRank, which splits documents into term-centric contexts for each query term. DeepRank constructs a tensor incorporating the word representations of the query and query-centric context along with their interactions. This tensor is then processed through a measurement network, often based on CNN [25] or 2D-GRU [50], to produce a representation of local relevance. The global relevance score is ultimately calculated using an aggregation network, showcasing the ability of PLMs to distill complex textual information into actionable scores. Hui et al. [18] proposed PACRR, a model influenced by neural models used in image recognition. PACRR uses a similarity matrix between a query and a document as input, with multiple CNN kernels to capture query-document interactions. Building upon PACRR, Hui et al. [19] developed CO-PACRR, a lightweight contextualization model that averages word vectors within a sliding window, appending the similarities to those of the PACRR model. These developments highlight the versatility of PLMs in adapting to diverse IR requirements.

Transformer-based models, such as BERT [9], have been particularly effective. They leverage attention mechanisms, pre-trained on large scale textual data, enabling a deeper understanding of the semantics embedded within queries and documents. The success of BERT in various NLP tasks, including IR, can be attributed to its capacity to obtain contextualized understanding that account for the surrounding text. It can be classified into three categories of BERT-based IR methods: interaction-based approach, representation-based approach and late-interaction based approach. The first kind is also called cross-encoder, where the query and passage are concatenated and inputted to the PLM or LLM. Nogueira and Cho [35] proposed using BERT as a cross-encoder for passage re-ranking by fine-tuning the model, achieving significantly higher results than earlier neural-IR models.

The second kind is also called dense retrieval models or bi-encoder. Karpukhin et al. [22] propose DPR for open-domain question answering, showing simply fine-tuning the question and passage encoders on existing question-passage pairs is sufficient to greatly outperform BM25. They also investigate various negative sampling strategies. Similarly, Reimers and Gurevych [43] propose Sentence-BERT, which use siamese and triplet network structures to derive semantically meaningful sentence embeddings. Later works focus more on the hard negative mining or domain adaptation for the bi-encoders, such as ANCE [52], SimANS [58] and DoDress [29].

ColBERT [23], a representative approach of the third category, introduces a late interaction architecture that independently encodes each token in the query and the document using BERT, and then employs a cheap yet powerful interaction step to model fine-grained similarity. Later, ColBERTv2 [46] is proposed, which combines distillation from a cross-encoder with hard-negative mining to boost effectiveness. It also introduces a residual compression mechanism to reduce the storage cost of token-level representations. To further improve efficiency,

PLAID [45] builds on ColBERTv2 with a performance-optimized engine that leverages centroid interaction and pruning to reduce search latency by up to 45 \times on CPU and 7 \times on GPU, while maintaining high retrieval quality.

2.2 Long Document Re-ranking

Dealing with long documents presents a significant challenge for Transformer-based models due to their quadratic complexity. Previously, this complexity arises from the self-attention mechanism, which becomes computationally prohibitive as input length increases, as well as the design of positional embeddings. To overcome these limitations, researchers have explored various strategies to enable Transformer-based models to process long documents effectively. For instance, Dai et al. [8] proposed a model that incorporates left-to-right recurrence across transformer windows, featuring a segment-level recurrence mechanism combined with a new positional encoding method. Beltagy et al. [2] propose the Longformer with an attention mechanism that combines local and global information, making it easy to process documents of thousands of tokens or longer. Child et al. [4] proposed several sparse factorizations of the attention matrix that reduce its computational complexity from quadratic $O(n^2)$ to $O(n\sqrt{n})$. Zaheer et al. [55] introduced BigBird, which integrates local and global attention mechanisms along with random sparse attention to handle long sequences. Kitaev et al. [24] addressed the challenge of efficient self-attention by computing it only between similar tokens, identified through locality-sensitive hashing.

Similarly, for IR dealing with long documents, one line of research uses modified Transformer architecture. Hofstätter et al. [14] introduced TKL, which employs local self-attention by using a sliding window over the document and limiting the attention to that window, addressing the challenge of processing long documents. Jiang et al. [21] proposed the Query-Directed Sparse Transformer (QDS-Transformer), which introduces sparsity into the self-attention mechanism by combining local windowed attention with query-directed global attention. Experimental results demonstrate that the QDS-Transformer consistently outperforms previous methods, showing robust advantages across various tasks. However, these modified attention mechanisms still suffer from lower effectiveness and often require custom techniques or CUDA kernels for efficient sparse multiplication on GPUs [11, 21, 55].

Another line of approach involves breaking long documents into segments, known as passages, and independently processing these segments. Dai and Callan [7] propose segmenting documents into short, overlapping passages and using BERT to calculate either the first passage's relevance score, the max score of the passages, or the sum of all passage scores. However, it either lose information or is a little coarse-grained. Later, Li et al. [27] propose PARADE model, which utilizes Transformer encoder layers, to combine query-passage relevance signals obtained with BERT, for query-document relevance score. The model shows significant improvements compared with baselines. However, it suffers from high computational costs with high GPU memory requirement, as it need to combine the block level signals meanwhile to the Transformer layers, and each query-block pair is processed by BERT model.

One step further was achieved by approaches aiming to select key blocks. Hofstätter et al. [13] propose the IDCM approach. Firstly a lightweight Efficient Student Model (ESM) filters out non-relevant passages, and then a more expensive Effective Teacher Model (ETM), like BERT, evaluates the selected passages separately. The ESM is trained using knowledge distillation. Final query-document relevance scores are calculated using a weighted sum of passage scores. The ICL model [28] extends the late-interaction approach to long document retrieval by obtaining a passage representation for each passage in a long document with multi-task learning. Then the representation is used fast intra-passage ranking. Late interaction is then applied to the top-ranking passages to derive document relevance scores. Experimental results demonstrate the effectiveness. Li et al. [30] propose KeyB approach, also addresses long document re-ranking by first applying local pre-ranking using traditional IR scoring functions like BM25, or learned scoring methods. The top relevant blocks are then aggregated and processed by a BERT-based model. Unlike IDCM, KeyB processes concatenated blocks as a unified input and

shows better performance on datasets like TREC 2019 DL. KeyB allows for a flexible integration with existing models, enhancing scalability. In this paper, we focus on the interaction-based KeyB approach and want to incorporate it with LLMs to see whether in LLMs era, the selecting key block approach is also helpful and can improve the results.

2.3 Reranking with Large Language Models

The utilization of LLMs for reranking has emerged as a promising direction in IR. Unlike earlier models, LLMs, with their vast parameter counts, can potentially grasp the nuances of documents and complex queries. Sun et al. [48] first investigate prompting ChatGPT with two existing strategies [31, 44] but observe limited performance. Then they propose an alternative instructional permutation generation approach, instructing the LLMs to directly output the permutations of a group of passages, with a sliding window strategy to address context length limitations. Results demonstrate that GPT-4, equipped with zero-shot instructional permutation generation, surpasses supervised baselines across nearly all datasets.

The RepLLaMA and RankLLaMA models [34], exemplify the potential of LLMs in IR. They leverage LLMs directly to serve as components in the widely used multi-stage text ranking pipeline. They fine-tune the open-source Llama-2 model as a dense retriever (RepLLaMA) and a pointwise reranker (RankLLaMA). Through a straightforward training regime, these models exhibit strong zero-shot effectiveness and show that finetuned LLM retrieval models outperform smaller models. Their results show that compared to directly prompting LLMs to generate permutations [48], fine-tuning LLMs as rerankers can be more effective. However, in terms of document ranking task, e.g., TREC 2019 DL document ranking, the results do not surpass the BERT-based KeyB approach [30]. Zhang et al. [56] propose a two-stage progressive paradigm to adapt LLMs to text ranking. The first stage continuously pretrains LLMs with relevant text pairs on large weakly supervised corpus. The second stage enhances text ranking performance using supervised finetuning and optimized loss functions. Liu et al. [32] propose PERank, leveraging the single passage embedding as a good context compression for efficient listwise passage reranking. They directly input passage embeddings into LLMs and employ listwise learning to rank loss for training. Experimental results demonstrate that it achieves comparable ranking performance to uncompressed methods while improving inference efficiency. However, this approach requires obtaining passage embeddings and dynamically adjusting the decoding space, which increases architectural complexity and memory usage.

In conclusion, most of these approaches focus on passage retrieval tasks rather than on long-document ranking. RankLLaMA experiment on TREC 2019 DL document reranking task, but the results are lower than KeyB with BERT model. In this paper, we naturally follow the standard RankLLaMA approach and want to see if selecting key block approach is also important in the LLM era and can enhance the results.

3 Attention Analysis: Why Block Selection Still Matters

With the advent of PLMs like BERT, IR systems have seen substantial improvements in document ranking accuracy. Among these, re-ranking models, often referred to as cross-encoders, harness the power of fine-tuned PLMs or decoder-only LLMs for downstream IR tasks. Despite the impressive performance of decoder-only LLMs like RankLLaMA, the inner workings of these LLMs, specifically how they assess and rank the relevance of passages, remain underexplored.

3.1 Attention Heatmaps of Specific Examples

To shed light on this and answer **RQ1**, we propose first analyzing the attention heatmaps of the RankLLaMA model with several specific examples, which has been fine-tuned on the MSMARCO passage ranking dataset¹. Clark et al. [5] propose a similar investigation for BERT and find a significant portion of BERT’s attention is

¹available at: <https://huggingface.co/castorini/rankLlama-v1-7b-lora-passage>

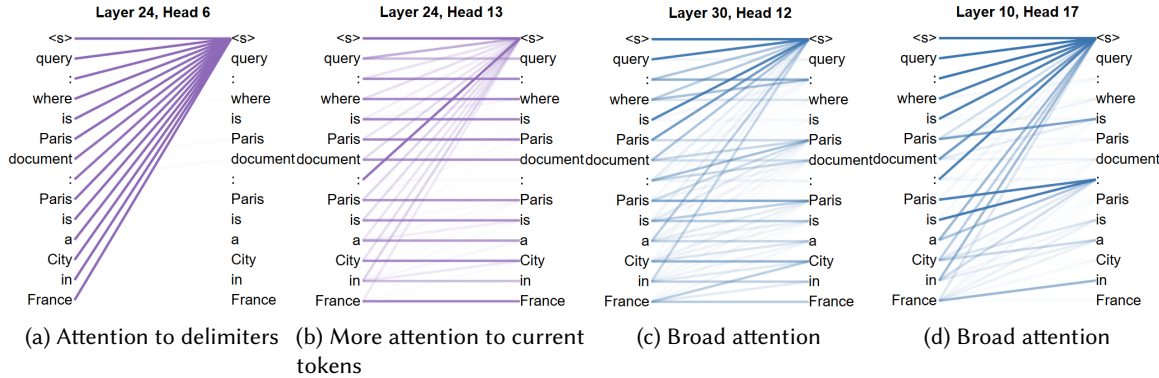


Fig. 1. Attention heads that attend to delimiters, current tokens or attend broadly.

focused on the delimiter token, and certain attention heads align well with linguistic features such as syntax and coreference. However, recent LLMs are uni-directional and decoder-only, especially for the IR focused LLMs, and may display a different behavior regarding how tokens attend to each other. We used the BertViz tool [49] to explore these attention patterns in the decoder-only LLM RankLLaMA when processing various query-passage pairs.

We begin with a simple and arbitrary text pair: the query text is "where is Paris", and the document text is "Paris is a city in France". With the format "query: [query] document: [document]", after Llama2 tokenizer, the input tokens are: '<s>', '_query', ':', '_where', '_is', '_Paris', '_document', ':', '_Paris', '_is', '_a', '_City', '_in', '_France'. We check several attention heads which are shown in Fig. 1, Fig. 2, Fig. 3 and Fig. 4. To help showing weak attention weights, the last three figures are sharpened. Our findings are summarized in the following points:

- Attention to delimiter, current and broad tokens: Similar to [5] in BERT, we observe that a substantial portion of attention is directed towards the delimiter token <s>, e.g., Fig. 1a. Clark et al. [5] speculate that attention over the <s> delimiter tokens might be used as a sort of "no-op", and we conjecture that the attention over the beginning <s> is also "no-op" for IR scenario. Besides, we also observe a small amount of attention is directed towards the current token (Fig. 1b), and that some attention heads attend broadly over all tokens (Fig. 1c, Fig. 1d), which is consistent with [5].
- Attention focusing on relevant tokens: Beyond delimiter-focused or self-focused heads, we observe several attention heads that directly capture semantic relations between relevant tokens in the query and document. In particular, as shown in each above three subfigures in Fig. 2, Fig. 3, and Fig. 4, these relevance-focused heads consistently highlight key cross-token alignments: for head 23 in layer 1, tokens such as "Paris" and "France" in the document primarily attend to corresponding relevant tokens in both query and document segments; for head 25 in layer 8, tokens "Paris" and "France" focus strongly on the query token "Paris"; for head 24 in layer 31, similar alignment between query and document relevance tokens is also preserved. These patterns suggest that a subset of attention heads are able to capture fine-grained token-level relevance signals, forming direct associations between query intents and document content—an essential mechanism underlying accurate relevance estimation.
- Attention with irrelevant information: To investigate the effect of irrelevant tokens, we insert unrelated content such as "An apple is a fruit" into the document. This setting is illustrated in the three subfigures in Fig. 2, Fig. 3, and Fig. 4. The attention head 25 in layer 8 (Fig. 3e) effectively suppresses the irrelevant



Fig. 2. Example attention map of layer 1 head 23, that potentially is capturing the relevance information.

content, maintaining strong attention on the relevant query token “Paris.” This head appears to filter out the noise (e.g., apple) and prioritize query-relevant content.

In contrast, head 23 in layer 1 (Fig. 2e) continues to exhibit broad attention across all tokens. Although the attention may be weak, it reveals that the head does not clearly distinguish between relevant and irrelevant content. Similarly, head 24 in layer 31 (Fig. 4e) shows that the token “Paris” in the document attends not only to the query token “Paris” but also weakly to irrelevant tokens such as “apple,” “is,” and “a.”

Importantly, except for head 25 in layer 8, **the introduction of irrelevant tokens leads to a noticeable reduction in the attention weight toward the query token “Paris.”** For instance, in Fig. 2f and Fig. 4f, the attention from the final document token “France” to the query token “Paris” becomes weaker after inserting irrelevant information.

To support this observation quantitatively, Table 1 presents the measured attention scores from “France” to “Paris” in the query across the three heads. All heads exhibit decreased attention scores following the insertion of irrelevant tokens. Notably, while the decline for Layer 8 Head 25 is mild, the other two heads show substantial drops. This degradation may impair the model’s ability to correctly assess the relevance between document and query, which is particularly critical in information retrieval scenarios.

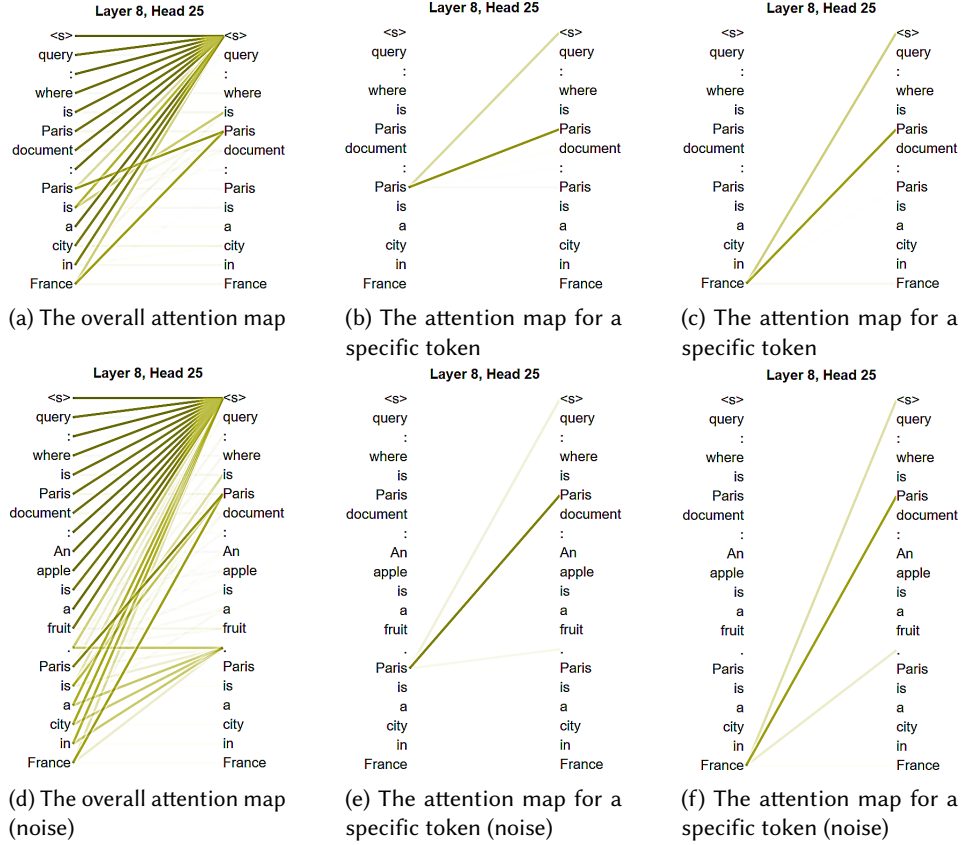


Fig. 3. Example attention map of layer 8 head 25, that potentially is capturing the relevance information.

Table 1. The attention weights between “France” to “Paris” in the query when inserting noise tokens.

	Layer 1 Head 23 (Fig 2)	Layer 8 Head 25 (Fig 3)	Layer 31 Head 24 (Fig 4)
no noise tokens	0.2097	0.6500	0.1296
with noise tokens	0.1154 (\downarrow 44.97%)	0.6492 (\downarrow 0.12%)	0.0858 (\downarrow 33.80%)

These irrelevant tokens will inevitably result in noisy information in the representation of the last token, which is the basic building block for computing the relevance score for RankLLaMA.

3.2 Aggregated Attention Heatmaps Across Examples

The previous section illustrates attention behaviours on individual examples. To investigate whether these patterns generalize across real-world long documents, we conduct a dataset-level aggregation analysis. Specifically, we sample 500 query-relevant document pairs from the TREC DL19 document ranking’s development set (MS

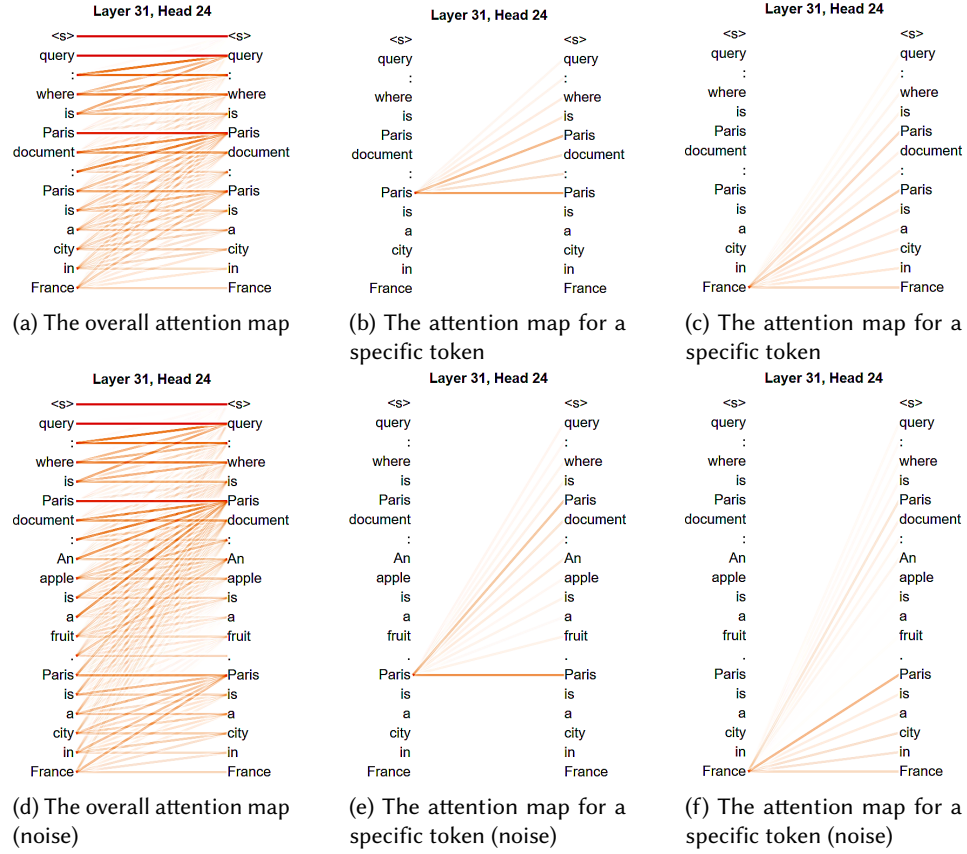


Fig. 4. Example attention map of layer 31 head 24, that potentially is capturing the relevance information.

MARCO) [6]. The RankLLaMA model fine-tuned for document-level reranking² is used for evaluation. All documents are truncated to 1200 tokens.

For each example, we compute the average attention scores from document tokens to query tokens across all heads in every layer. The attention scores are then averaged across the sampled set to produce an overall heatmap summarizing attention behaviour across layers and heads.

To assess robustness against irrelevant context, we also create two additional test settings. For each query-relevant document pair, we randomly sample a negative document, extract its first 800 tokens as noise, and insert the noise either before or after the relevant document. The aggregated attention heatmaps under these two noise injection settings are similarly computed. The resulting heatmaps for the clean and noisy cases are shown in Fig. 5.

3.2.1 Findings. As shown in Fig. 5a, certain heads—primarily located in the beginning and middle layers, as well as several heads in the final layers—exhibit strong attention from document tokens to query tokens, aligning with relevance-focused behaviour observed earlier. However, when noise is inserted, both Fig. 5b and Fig. 5c display a general attenuation of attention scores, indicating that irrelevant content weakens the focus on relevant tokens.

²<https://huggingface.co/castorini/rankllama-v1-7b-lora-doc>

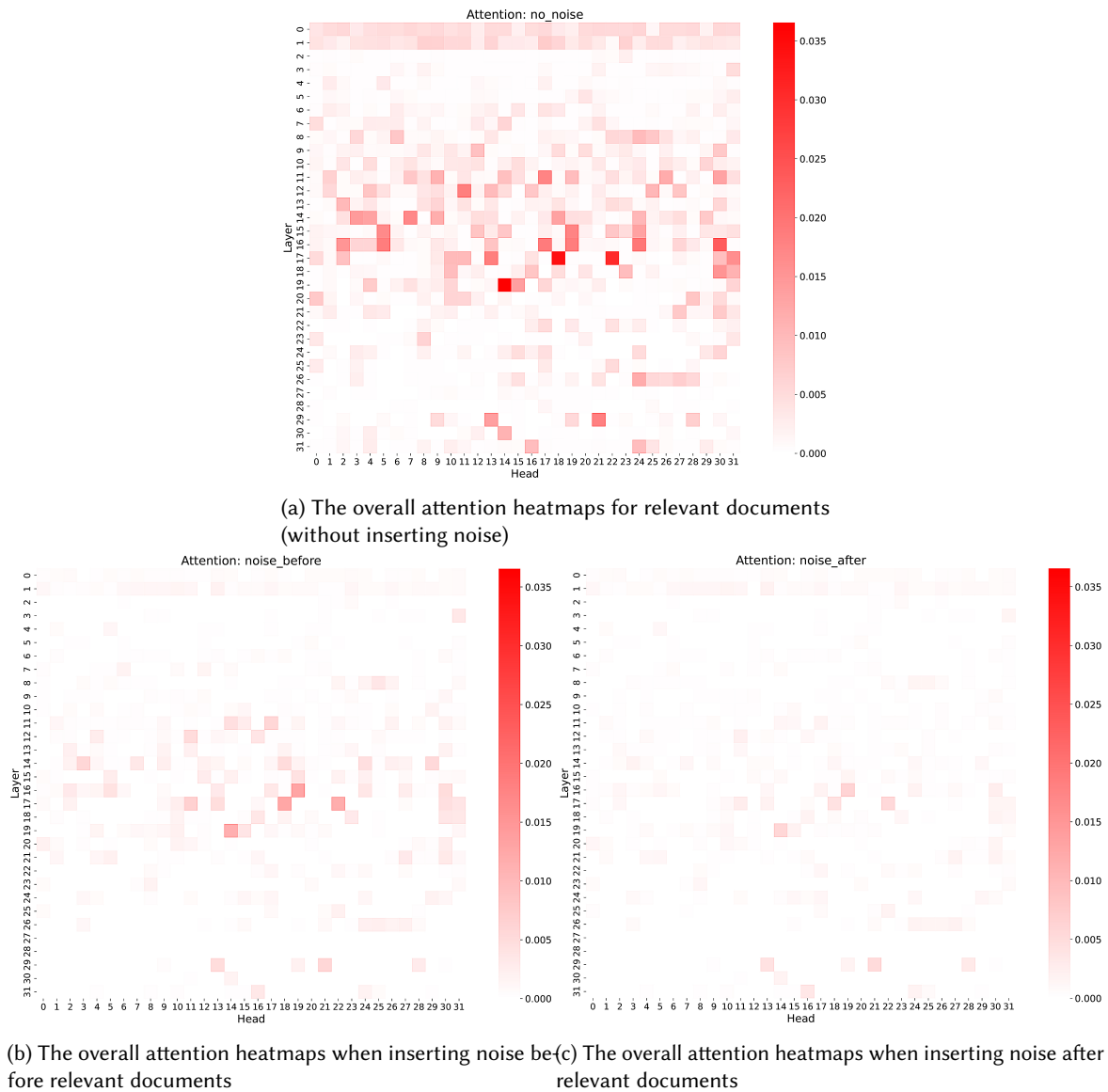


Fig. 5. The overall attention heatmaps across samples, comparing with inserting noise tokens.

Notably, inserting noise *after* the relevant content appears to cause greater attention dispersion, likely because the model processes text autoregressively from left to right.

These aggregated patterns confirm that a fraction of attention heads identify relevance signals, and that irrelevant text can dilute these signals, motivating selective block extraction before LLM reranking.

3.3 Quantitative Analysis with Attention-Relevance Alignment Score (ARAS) and Positive Correlation Rate (PCR)

To complement the above qualitative attention observations and provide a more systematic and quantitative understanding of how LLM rerankers behave (addressing **RQ1**), we propose two evaluation metrics: the **Attention-Relevance Alignment Score (ARAS)** and the **Positive Correlation Rate (PCR)**. These metrics aim to measure how well the model's attention aligns with true relevance signals in long documents.

3.3.1 Metric Definitions.

- Attention weight per chunk: Given a query-document pair (q, d) , we first segment the document d into M non-overlapping chunks $\{C_1, C_2, \dots, C_M\}$, where each chunk contains a fixed number of tokens. For a given attention head and layer, let $\mathbf{A} \in \mathbb{R}^{L \times L}$ denote the attention matrix for the entire input sequence of length L .

Let $Q = \{q_1, q_2, \dots, q_{|Q|}\}$ represent the token indices of the query portion in the input sequence. Then, for each document chunk C_i (corresponding to token indices $\{c_{i,1}, \dots, c_{i,K}\}$), we compute its average attention weight toward the query tokens as:

$$\text{AttentionWeight}(C_i) = \frac{1}{K} \sum_{t \in C_i} \frac{1}{|Q|} \sum_{j \in Q} \mathbf{A}_{t,j}$$

This reflects how much attention the document chunk as a whole assigns to the query tokens.

- Relevance score per chunk: For each chunk C_i , we estimate its relevance with respect to the query using an external cross-encoder model³ which serve as an approximate "ground-truth" relevance score:

$$\text{RelevanceScore}(C_i) = \text{CrossEncoder}(q, \text{text}(C_i))$$

where $\text{text}(C_i)$ denotes the surface text of chunk C_i .

- Attention-Relevance Alignment Score (ARAS): For each query-document pair (q, d) , the ARAS is defined as the Spearman rank correlation coefficient between the attention weights and relevance scores across all chunks:

$$\text{ARAS}(q, d) = \text{Spearman} \left(\{\text{AttentionWeight}(C_i)\}_{i=1}^M, \{\text{RelevanceScore}(C_i)\}_{i=1}^M \right)$$

This measures how well the ranking induced by attention weights aligns with the ranking of relevance scores across chunks. For reporting, we compute the overall mean ARAS across the samples:

$$\overline{\text{ARAS}} = \frac{1}{N} \sum_{j=1}^N \text{ARAS}(q_j, d_j)$$

This average ARAS indicates the typical alignment strength per query-document pair.

- Positive Correlation Rate (PCR): Given a collection $\mathcal{D} = \{(q_j, d_j)\}_{j=1}^N$ of N query-document pairs, we compute PCR as the proportion of pairs whose ARAS is positive:

$$\text{PCR} = \frac{1}{N} \sum_{j=1}^N \mathbb{I}(\text{ARAS}(q_j, d_j) > 0)$$

where $\mathbb{I}(\cdot)$ is the indicator function. PCR reflects how consistently attention correlates positively with relevance across the dataset.

³<https://huggingface.co/cross-encoder/ms-marco-MiniLM-L6-v2>

ARAS focuses on the alignment strength between attention and relevance for individual query-document pairs, while PCR reflects alignment stability across the dataset. Together, these metrics offer both instance-level and corpus-level interpretability.

3.3.2 Experimental Setup. We conduct controlled experiments on 500 query-relevant document pairs sampled from the same development set (MS MARCO) as Section 3.2. Each document is truncated to 1200 tokens, and segmented into 64-token chunks for analysis. The ARAS and PCR metrics are then computed across three representative attention heads previously identified: Layer 1 Head 23, Layer 8 Head 25, and Layer 31 Head 24.

To simulate long irrelevant contexts, we insert 800 to 1800 noise tokens either before or after the relevant document content, allowing us to test attention stability under varying noise levels.

3.3.3 Results and Findings.

Layer 1, Head 23. Under clean input, ARAS achieves 0.349 and PCR reaches 83.9%, suggesting moderate attention-relevance alignment at shallow layers. However, performance degrades significantly as noise is inserted, particularly when noise follows the relevant content. ARAS drops to negative values and PCR falls below 50% under heavy noise, indicating this head is highly sensitive to positional disruptions.

Layer 8, Head 25. This head shows the strongest relevance alignment: baseline ARAS reaches 0.602 and PCR 96.6%. Although both metrics decline with added noise, PCR remains relatively stable (above 70%), suggesting that this mid-layer head is better at resisting irrelevant information. Nevertheless, ARAS still declines sharply as more noise accumulates, indicating that although the head consistently identifies relevant regions, the precision of its attention distribution becomes less aligned with true relevance as noise increases.

Layer 31, Head 24. This deep-layer head exhibits relatively weak alignment, with a baseline ARAS of 0.284 and PCR of 79.6%. As with earlier heads, both metrics decline in the presence of noise. Although its performance degrades more slowly than Layer 1, it still suffers substantial drops under high noise levels—ARAS falls below 0.1 and PCR drops to approximately 56%.

Overall Observations. Across all heads, inserting irrelevant tokens *after* the relevant content consistently causes more severe alignment degradation than inserting noise *before*, likely because autoregressive LLMs encounter relevant content later, reducing the usable attention capacity.

3.4 Summary: Implications for Long Document Retrieval

These findings provide a direct answer to **RQ1**, showing that while certain attention heads do exhibit relevance-focused behaviors, their ability to preserve this alignment diminishes substantially when irrelevant content accumulates. This degradation is especially pronounced when noise appears later in the sequence, likely due to the left-to-right processing nature of decoder-only LLMs such as RankLLaMA.

These results reinforce the need for explicit block selection before LLM reranking—not only to reduce computational overhead, but also to preserve attention focus, mitigate distraction from irrelevant text, and prevent attention dispersion. This insight validates the core motivation behind KeyB2: block selection remains necessary even in the era of large language models. By selecting and ranking the most relevant content blocks, we enable LLMs to concentrate attention on relevant information, thereby improving both retrieval effectiveness and computational efficiency.

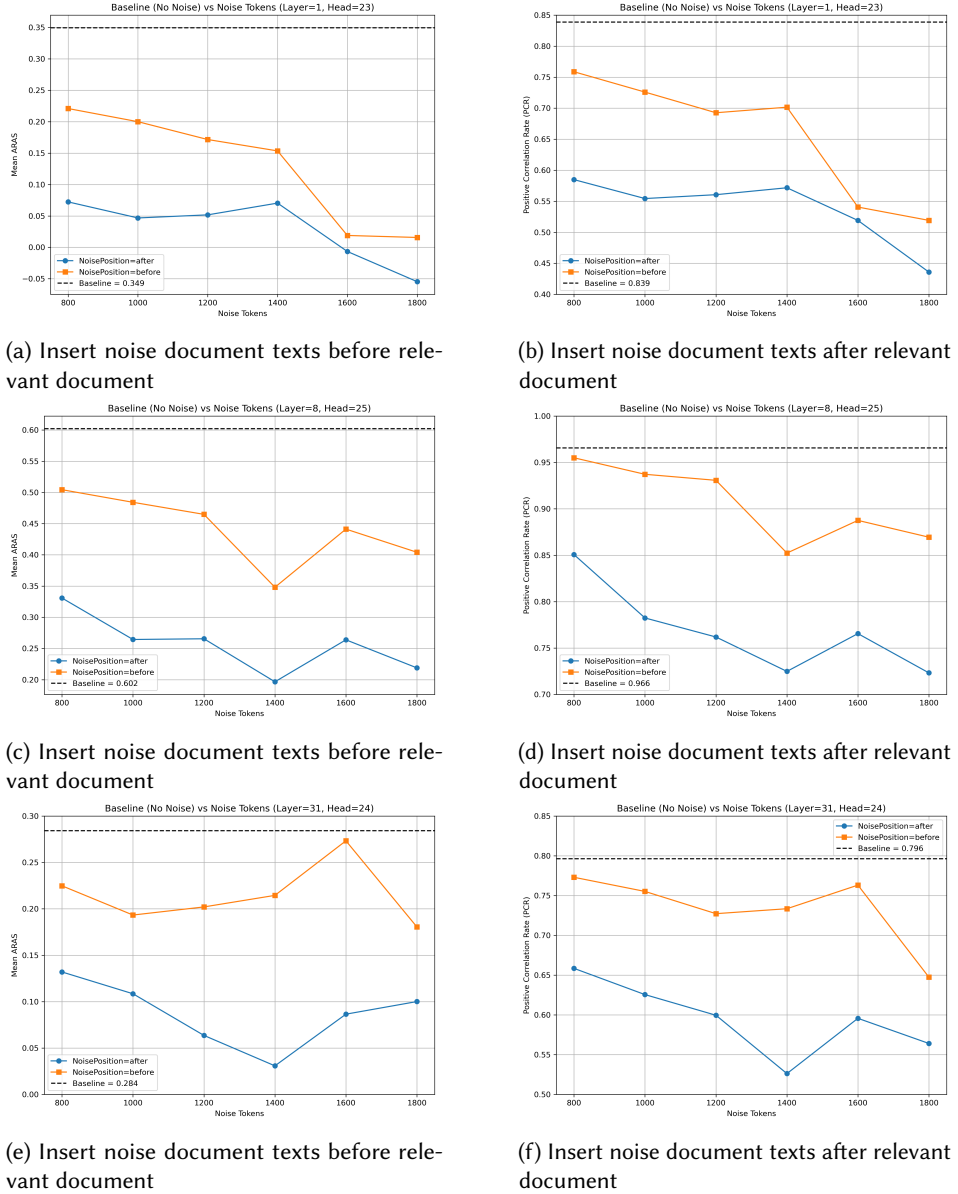


Fig. 6. Mean ARAS scores and positive correlation rates for different layers across various noise lengths and different noise insertion positions. Baseline is the score without inserting noise tokens.

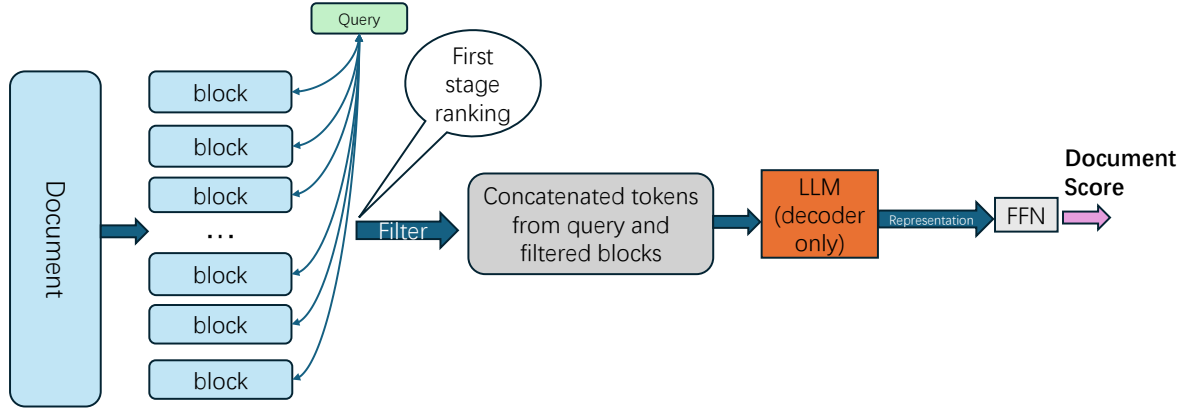


Fig. 7. The architecture of proposed KeyB2 approach.

4 KeyB2 Framework: Block Selection Enhanced LLM Reranking

4.1 Recap of KeyB Framework and Differences in KeyB2

The KeyB framework [30] was originally proposed to address long-document ranking challenges by applying a two-stage architecture: (1) selecting salient blocks from documents, and (2) performing relevance estimation on the selected blocks. In KeyB, block selection is conducted using either BM25 scoring or a the cross-encoder itself. The downstream reranker in KeyB is a BERT-based cross-encoder, which jointly models the query and selected document blocks within 512 tokens.

The fundamental design insight of KeyB is that long documents typically contain many irrelevant sections, and identifying relevant blocks prior to full interaction modeling can improve both ranking effectiveness and computational efficiency. In this work, we extend this block selection paradigm to modern large language models (LLMs), resulting in the KeyB2 framework. While KeyB2 retains the similar select-then-rerank architecture as KeyB, it introduces several key differences and enhancements:

- Architectural adaptation to autoregressive LLMs: KeyB2 replaces KeyB’s bidirectional BERT reranker with decoder-only LLMs (e.g., Llama 2/3), which necessitates a different scoring mechanism. Instead of [CLS] token pooling, KeyB2 follows the RankLLaMA approach: the entire input sequence (query + selected blocks) is encoded autoregressively, and the final hidden state is passed through a linear layer to obtain the relevance score. This design enables fine-grained modeling of long input sequences while adapting to the left-to-right generation nature of LLMs.
- Expanded block selectors: KeyB2 extends the block selection module to support three types of selectors: BM25, neural cross-encoders, and bi-encoders. This design enables flexible trade-offs between selection accuracy and computational efficiency, accommodating diverse deployment constraints and retrieval scenarios.
- Attention-based design motivation: Our attention analysis on LLM rerankers (Section 3) reveals that feeding inputs with appended irrelevant content—can lead to significant attention dispersion and misalignment. These findings highlight the need for explicit block selection to mitigate such attention degradation, reinforcing the design rationale behind KeyB2.

Overall, KeyB2 preserves the core idea of KeyB while extending the framework to the LLM era with stronger backbones, richer selector choices, and deeper empirical analysis. The systems we propose, illustrated in Figure 7,

are based on block selection mechanisms using fast models as standard IR models or PLMs, followed by LLMs and trained as rankers. Next we introduce the document segmentation approach, followed by three distinct block pre-ranking methods, including a novel one, and concludes with an aggregation of the top-scoring blocks.

4.2 Passage Segmentation Approach

When reading a document for assessing its relevance with respect to a given query, humans tend to segment the document into pieces prior to scan each piece for assessing its relevance [10]. Inspired by this, passage or block segmentation methods have become popular in IR. We use in this paper the CogLTX [10] block decomposition method, which have been applied with success on several NLP tasks and which sets different costs for different punctuation marks with the aim to segment in priority on strong punctuation marks such as "." and "!", making it close to the sentence segmentation procedure used by humans. CogLTX segments each long text D into a sequence of blocks $[b_1 \dots b_n]$ using dynamic programming. This process ensures that the length of each block does not exceed a predefined maximum value B ; in our implementation, $B=63$, which is the same as the setting in [30].

Furthermore, to be consistent with the final LLM-based IR ranker, we use different tokenizers depending on the IR ranker used: the Llama2 tokenizer is used when the IR ranker is Llama2 whereas the Llama3 tokenizer is used when the IR ranker is Llama3. Last but not least, for Chinese documents, since in Chinese, marks imported from Europe are fullwidth instead of halfwidth like their original European counterparts⁴. So in Chinese, the punctuations are different with English in terms of: comma, period, exclamation mark and question mark, and we incorporate various Chinese punctuation marks into CogLTX. This ensures more effective separation of Chinese sentences.

4.3 Local ranking approaches for KeyB2

After segmenting the long document into blocks, the keyB2 model efficiently calculate the local relevance. This step should be significantly faster than using LLMs. The IR community has evolved in the past decades, from bag of words approaches to using neural networks including Transformer based networks. Different IR approaches can be plugged in the KeyB2 model. In this paper, we adopt three different approaches: they are BM25, cross-encoder and bi-encoder models. These three approaches are widely used in academia and industries.

4.3.1 KeyB2-BM25. BM25 is a term-matching retrieval model that extends the classic TF-IDF formulation. While both methods down-weight ubiquitous terms through inverse document frequency, BM25 further (i) applies a sub-linear saturation function to term frequency, and (ii) introduces a length-normalization factor that penalizes disproportionately long documents. These two mechanisms are controlled by tunable hyper-parameters k_1 and b , enabling BM25 to balance term frequency impact and document length effects more effectively than TF-IDF, and thus to deliver stronger empirical performance in long-document ranking tasks.

Given a query and a block, the Retrieval Status Value (RSV) is calculated as below:

$$RSV(q, blk)_{BM25} = \sum_{w \in q \cap blk} IDF(w) \cdot \frac{tf_w^{blk}}{k_1 \cdot (1 - b + b \cdot \frac{l_{blk}}{l_{avg}}) + tf_w^{blk}},$$

in which tf_w^{blk} corresponds to the number of occurrences of word w in the block blk and $IDF(w)$ to the inverse document frequency of word w . In this paper, we use the scikit-learn [39] package to calculate the IDF dictionary with IDF smoothing. $IDF(w)$ is defined by:

$$IDF(w) = \log \frac{N + 1}{df_w + 1} + 1,$$

⁴https://en.wikipedia.org/wiki/Chinese_punctuation

where N and df_w are added one with default scikit-learn smooth IDF setting. The added 1 after the fraction, makes sure terms with zero IDF don't get suppressed entirely. Besides, l_{blk} is the length of block, l_{avg} the average length of the blocks in d , and k_1 and b two hyperparameters of BM25.

For Chinese documents, word w is recognized using the Jieba⁵ Chinese text segmentation tool to obtain meaningful terms.

4.3.2 KeyB2-cross. For each block denoted as b_i , to calculate its relevance with the query, we also can use a cross-encoder model, which should be efficient since the length of each block is limited. Since the block number is relatively large, this model should be relatively fast. We use pre-trained language models (PLMs) like BERT [9] as the cross-encoder, with a typical number of parameters ranging from dozens of millions to hundreds of millions, which is one to two orders of magnitude smaller than the one of LLMs. Denoting by b_i the i^{th} block and b_i^{cls} the corresponding query-block representation, one has:

$$b_i^{cls} = \text{PLM}([\text{CLS}], q_tokens, [\text{SEP}], b_i_tokens),$$

where PLM is a pre-trained language model like BERT, q_tokens are the tokens of the query and b_i_tokens are the tokens of the block. A linear layer is then used to generate the query-block relevance score:

$$RSV(q, b_i) = W b_i^{cls},$$

where W is the learnable weights of a feedforward neural network.

4.3.3 KeyB2-bi. The previous subsection uses a cross-encoder to identify the query-block relevance. Although cross-encoders have shown their effectiveness, they have the drawback of high computational latency since the concatenated query-block tokens should be calculated online. On another side, bi-encoders are another kind of neural-IR approaches which are very efficient because the block representations can be calculated offline (also called dense retrieval). Besides, compared with BM25, they have the ability to capture the semantic relevance information. Normally, the query encoder and passage/block encoder can be shared, and in this paper, we follow this paradigm: a same encoder is used for queries and blocks.

Given a query or a block, the bi-encoder model encodes the tokens of the query or the tokens of the block into a high dimensional representation:

$$\begin{aligned} q^{cls} &= \text{PLM}([\text{CLS}], q_tokens), \\ b_i^{cls} &= \text{PLM}([\text{CLS}], b_i_tokens). \end{aligned}$$

Then the retrieval status value is calculated by either:

$$RSV(q, b_i) = q^{cls} \cdot b_i^{cls},$$

or

$$RSV(q, b_i) = \cos(q^{cls}, b_i^{cls}).$$

4.4 Aggregating the Local Relevance

To aggregate the different blocks deemed relevant to the query, the KeyB2 approach selects the most relevant blocks given a query and aggregate the tokens of these blocks with the query in order to generate the overall document relevance score using LLMs. More precisely, given the scores of blocks: $S = [s_1 \dots s_n]$, and the max combined block token limitation max_b_t , the selected top k blocks from the list S are $B_r = [b_{r_1}, b_{r_2}, \dots, b_{r_k}]$, which satisfy:

$$\sum_{i=1}^k L(b_{r_i}) \geq max_b_t, \quad (1)$$

⁵<https://github.com/fxsjy/jieba>

and

$$\sum_{i=1}^{k-1} L(b_{r_i}) < \text{max_b_t}. \quad (2)$$

The tokens for the newly concatenated document are:

$$\text{Sort}_{\text{index}}(B_r) = [b^1 \dots, b^i, \dots, \text{trunc}(b^k)], \quad (3)$$

where b^i is the i th block in the top k scoring blocks B_r , after having re-ranked the list according to their original indexes in the original document, and $\text{trunc}(b^k)$ means the last block is truncated according to max_b_t , similar to [30]. This step ensures the top k blocks are re-ordered according to their original appeared locations in the document, to allow a coherent meaning and structure.

Finally, the step goes to calculating the RSV between the query and $\text{Sort}_{\text{index}}(B_r)$, in this paper, the KeyB2 model follows RankLLaMA approach to calculate the relevance score. The formatted input tokens are:

$$\text{input} = \text{'query: } \{Q\} \text{ document: } \{\text{Sort}_{\text{index}}(B_r)\}',$$

and the RSV is:

$$\text{RSV}(Q, D) = \text{Linear}(\text{Decoder}(\text{input})[-1]) \quad (4)$$

5 Experimental Settings

From this section, we evaluate the proposed approach on various datasets and compare it with baseline models, mainly aiming at addressing **RQ2**, **RQ3** and **RQ4** as introduced in Section 1.

5.1 Datasets

Since this paper focuses on document ranking, the datasets should be relatively long. In this paper, we use 4 datasets:

- TREC 2019 DL document reranking task [6] is the first dataset. The Deep Learning Track, introduced for TREC 2019, aims to study large data ad hoc ranking. It is the first track large human-labeled training datasets. It includes two tasks: document ranking and passage ranking. In this paper, we focus on the document reranking task.
- TREC 2023 DL document reranking task is further experimented on different models, whose corpus is based on MS MARCO v2, different with DL19's.
- Robust04⁶ is the third dataset, whose sources include Financial Times, Federal Register 94, FBIS, disk 5 and LA Times.
- MLDL Multilingual Long-Document Retrieval dataset [3] is the last dataset, and we use the MLDL-zh (Chinese) subset. The sources of MLDL-zh are Wikipedia and Wudao [54].

Table 2 summarizes key statistics of the datasets, including document genres, corpus sizes, test query counts, and average document lengths (using Llama2 tokenizer). Among them, MLDL-zh features the longest documents, while Robust04 primarily contains shorter newswire articles. These datasets offer a diverse experimental setting for evaluating KeyB2.

5.2 Baselines

We compare KeyB2 against several strong baselines, covering both traditional retrieval methods and advanced neural reranking models. The baseline configurations slightly differ across datasets.

⁶<https://trec.nist.gov/data/robust/04.guidelines.html>

Table 2. Datasets statistics

Dataset	genre	#documents	#test query	Avg. Num. of Tokens
TREC DL19 doc (MS MARCO)	Web Documents	3,213,835	49	1958
TREC DL23 doc (MS MARCO v2)	Web Documents	11,959,635	82	3782
Robust04	News Articles	528,030	250	741
MLDR-zh	Wikipedia + Wudao	200,000	800	12899

5.2.1 *Baselines on TREC DL 2019.* Following [30], we include a broad set of competitive baselines for TREC DL 2019, including:

- Traditional IR: BM25 implemented via Anserini [53].
- Neural IR models: CO-PACRR [19], TK [15], TKL [14], PARADE [26], RoBERTa-based aggregators (FirstP, MaxP) [33], and sparse attention models such as Sparse-Transformer [4], Longformer-QA [2], Transformer-XH [57], and QDS-Transformer [21].
- Previous SOTA reranking system: idst_bert_r1 [6].
- Previous key block selection models: IDCML [13] and KeyB [30].
- LLM-based reranker: RankLLaMA [34], along with our implemented variants RankLLaMA-MaxP and RankLLaMA-AvgP for segment-level score aggregation.

5.2.2 *Baselines on TREC DL 2023, Robust04, and MLDR-zh.* For these datasets, we compare the following unified set of baselines:

- BM25: implemented with Anserini for English datasets, and adapted with word segmentation for MLDR-zh.
- KeyB models: KeyB with BM25-based and BiB-based block selection, using either BERT or Chinese-BERT encoders depending on language.
- LLM-based reranker: RankLLaMA, RankLLaMA-MaxP, and RankLLaMA-AvgP.

5.2.3 *RankLLaMA-MaxP and RankLLaMA-AvgP.* To enable a similar comparison with the block-based design of KeyB2, we implement two extended variants of RankLLaMA that adopt the same document segmentation strategy as KeyB2. Each document is first divided into same blocks as KeyB2. The final document-level relevance score is obtained by aggregating the block-level scores: RankLLaMA-MaxP selects the highest block score, while RankLLaMA-AvgP averages all block scores. These two aggregation variants serve to contrast the simple score aggregation schemes against the *select-then-combine-then-evaluate* paradigm employed by KeyB2.

5.3 Experimental Design and Implementation Details

5.3.1 *Experimental Design.* To evaluate the proposed KeyB2 approach, we conduct experiments on multiple datasets with both fine-tuning scenarios and zero-shot transfer. All models except BM25 are experimented the reranking effectiveness. We first fine-tune the models on the TREC 2019 DL document ranking dataset and compare their performance with various baselines. To ensure fair comparison with RankLLaMA, which utilizes the Llama2⁷ 7B model, we initially fine-tune KeyB2 using the same Llama2 backbone, denoted as KeyB2(Llama2). To further investigate scalability, we additionally fine-tune KeyB2 on the Llama3⁸ 8B model, denoted as KeyB2(Llama3).

The KeyB2 framework supports three block selection strategies: BM25, bi-encoder, and cross-encoder. We train KeyB2 under all three selectors, resulting in variants such as KeyB2(Llama2)_{BM25}, KeyB2(Llama2)_{bi}, and

⁷<https://huggingface.co/meta-llama/Llama-2-7b-hf>

⁸<https://huggingface.co/meta-llama/Meta-Llama-3-8B>

KeyB2(Llama2)_{cross}. We further conduct additional fine-tuning experiments on the TREC 2023 DL dataset to test transferability across MS MARCO v1 and v2 collections.

For zero-shot evaluation, we directly apply the KeyB2 models trained on TREC 2019 DL to Robust04 without any additional fine-tuning. Finally, both KeyB2 and baseline models are fine-tuned on the Robust04 and MLDR-zh datasets to assess in-domain ranking performance. For all datasets, BM25 directly produces initial retrieval rankings, while all other models are evaluated as rerankers operating on candidate document lists [53].

5.3.2 Implementation Details. All models are implemented in PyTorch 2.4.0 with CUDA 11.8. All training and testing experiments are performed on a NVIDIA A100-40GB GPU unless otherwise noted.

(1) Training Data:

- TREC 2019 DL: 200K training triplets (query, positive, negative) sampled from `msmarco-doctrain-top100`⁹, based on MS MARCO v1. The `qrel` file is used to identify positives, together with the `top100` file to sample negatives from the top-100 retrieved documents, forming the training triplets.
- TREC 2023 DL: 200K triplets constructed from `docv2_train_top100.txt.gz`¹⁰, derived from MS MARCO v2. Triplet generation follows the same procedure as TREC 2019 DL.
- Robust04: 5-fold cross-validation is conducted, with each fold containing 40K triplets. Fold splits follow the CEDR data protocol¹¹. For each fold, positives and negatives are formed using the `train.pairs` and `qrel` file.
- MLDR-zh: 10,000 training queries, each paired with one labeled positive and one labeled negative document, as provided by the official dataset annotations.

(2) Training Configurations:

- For KeyB2 models, we apply LoRA [17] to efficiently fine-tune the large language models while freezing the backbone weights. LoRA parameters are set to $r = 32$ and $\alpha = 64$, with a batch size of 2 and gradient accumulation steps of 8, yielding an effective batch size of 16. The learning rate is fixed at 5×10^{-5} , with pairwise hinge loss [30], using AdamW optimizer with WarmupDecayLR scheduler, and FP16 mixed-precision training is applied throughout.
- For RankLLaMA, due to the longer input length (4096 tokens), the batch size is set to 1. We initially attempted fine-tuning RankLLaMA on an NVIDIA H20 GPU (96GB), but it encountered out-of-memory (OOM) errors. Eventually, RankLLaMA models were trained on an A100 using gradient checkpointing to fit into memory. All other hyperparameters are identical to KeyB2.
- For RankLLaMA-MaxP and AvgP, firstly same input tokens are used as RankLLaMA, then the tokens are segmented into same blocks are KeyB2 models. During training, max or average block score is used to represent document relevant score. All other hyperparameters are identical to KeyB2.
- For all KeyB(BERT) models, we follow the same training configuration as in [30], using a learning rate of 5×10^{-5} , batch size of 4, and gradient accumulation steps of 8, with pairwise hinge loss [30]. For English benchmarks (e.g., TREC DL19), we initialize from the `bert-base-uncased` model¹², and for the Chinese benchmark MLDR-zh, we use `bert-base-chinese`¹³ as the starting point.
- All models are trained with the same training data (triplets) for 1 epoch.

(3) Input Size Settings:

- Queries are truncated to a maximum of 32 tokens for all models.

⁹<https://microsoft.github.io/msmarco/TREC-Deep-Learning-2019.html>

¹⁰<https://microsoft.github.io/msmarco/TREC-Deep-Learning.html>

¹¹<https://github.com/Georgetown-IR-Lab/cedr/tree/master/data/robust>

¹²<https://huggingface.co/google-bert/bert-base-uncased>

¹³<https://huggingface.co/google-bert/bert-base-chinese>

Table 3. The cross-encoders and bi-encoders that are used in KeyB2 models for datasets with different languages (huggingface Transformer versions).

	TREC 2019, 2023 DL & Robust04	MLDR-zh
cross-encoder	cross-encoder/ms-marco-MiniLM-L-6-v2	BAAI/bge-reranker-base
bi-encoder	sentence-transformers/all-MiniLM-L6-v2	DMetaSoul/Dmeta-embedding-zh-small

- For KeyB and KeyB2, block selection reduces documents to 480 tokens, which reduce the input length to approximate 512 tokens.
- RankLLaMA directly consumes long input up to 4096 tokens, which means approximate 4096-32=4064 document tokens.

(4) Block Selection Pretrained Models: We utilize language-specific cross-encoders and bi-encoders as block selectors in KeyB2. The detailed model configurations and sources are summarized in Table 3.

(5) BM25 Implementation:

- For English datasets, BM25 is implemented using the Anserini tool [53] with default settings ($k_1 = 0.9$, $b = 0.4$). For KeyB2 with BM25 selector, we computed the IDF dictionary using scikit-learn on the TREC 2019 DL dataset, with parameters matching Anserini’s defaults.
- For Chinese dataset MLDR-zh, BM25 baseline is also implemented with Anserini with default settings. For KeyB2 with BM25 selector, as mentioned in Section 4.3.1, the sentences are separated into Chinese words. Other settings are the same as English datasets.

(6) Evaluation Metrics:

- TREC 2019 DL: NDCG@10 and MAP, following prior works [26, 30].
- TREC 2023 DL is the same as TREC 2019 DL.
- Robust04: We report P@10, P@20, NDCG@10, NDCG@20, and MAP to evaluate both precision and ranking depth.
- MLDR-zh: As each query has one positive document within 8 candidates, we report P@1 (first-rank accuracy), MAP (global ranking quality), and NDCG@8 (full list ranking consistency).
- All models report the reranking results with the metrics. Except Robust04, they rerank the official first-stage results, and on Robust04, they rerank the BM25 top 100 results from Anserini.

(7) Efficiency Measurement:

- Inference latency: Average reranking time for 100 candidate documents per query on a single A100 GPU.
- GPU memory consumption: Peak memory usage measured during fine-tuning (batch size 1 for both KeyB2 and RankLLaMA).
- Speed-effectiveness tradeoff: All models are compared based on their Pareto frontier of accuracy versus computational cost.

6 Experimental Results

6.1 Dataset-wise Effectiveness Results

Significant test: differences are verified with a paired t-test (p -value ≤ 0.05) is used for measuring significance in each table. Superscripts used in all tables for KeyB2 model are: R = significantly better than RankLLaMA; B = significantly better than KeyB(BERT) $_{BinB}^B$; † / * / ‡ = significantly better than the BM25 / bi-encoder / cross-encoder selector, respectively. Then we will show the results on the datasets.

Table 4. Experiment on TREC 2019 DL document reranking benchmark and comparison with sparse attention models and previous select blocks models. Results of KeyB(BERT), LLM part and KeyB2 models are newly trained in this study and other baseline results are taken from [30]. Best results are in **bold**.

TREC 2019 Deep Learning Track Document Reranking		
Model	NDCG@10	MAP
Baseline models		
BM25	0.488	0.234
CO-PACRR [19]	0.550	0.231
TK [15]	0.594	0.252
TKL [14]	0.644	0.277
RoBERTa (FirstP) [7, 33]	0.588	0.233
RoBERTa (MaxP) [7, 33]	0.630	0.246
PARADE [26]	0.655	0.280
Previous SOTA: idst_bert_r1 [6]	0.719	0.292
Sparse attention models		
Sparse-Transformer [4]	0.634	0.257
Longformer-QA [2]	0.627	0.255
Transformer-XH [57]	0.646	0.256
QDS-Transformer [21]	0.667	0.278
Select blocks models		
IDCM [13]	0.679	0.273
KeyB(PARADE5) _{BM25} [30]	0.672	0.280
KeyB(PARADE5) _{BinB} [30]	0.676	0.277
KeyB(PARADE5) _{BinB2} [30]	0.678	0.279
KeyB(BERT) _{BM25}	0.683	0.281
KeyB(BERT) _{BinB}	0.697	0.283
LLM		
RankLLaMA	0.701	0.288
RankLLaMA-MaxP	0.643	0.269
RankLLaMA-AvgP	0.654	0.264
KeyB2 models		
KeyB2(Llama2) _{BM25}	0.713	0.293 ^B
KeyB2(Llama2) _{cross}	0.730 ^{RB}	0.302^B
KeyB2(Llama2) _{bi}	0.710	0.293 ^B
KeyB2(Llama3) _{BM25}	0.718	0.293 ^B
KeyB2(Llama3) _{cross}	0.731^{RB†}	0.298 ^B
KeyB2(Llama3) _{bi}	0.711	0.296 ^B

Tables 4–7 list detailed scores for every baseline and all KeyB2 variants on five evaluation settings. Below we summarise, without yet interpreting the research questions, the main numerical facts for each dataset. All relative improvements are reported as percentages “%”, computed against the strongest baseline on the same dataset.

- TREC DL19: Table 4 shows that KeyB2(Llama2)_{cross} attains 0.730 NDCG@10 and 0.302 MAP. Compared with previous SOTA reranking system idst_bert_r1 [6] with NDCG@10 0.719 and MAP 0.292, the two KeyB2 with cross-encoder models consistently outperform it for both metrics, making KeyB2 models reach new SOTA results on TREC 2019 DL document reranking task. Compared with RankLLaMA (0.701

Table 5. Experiment on TREC 2023 DL document reranking benchmark and comparison with sparse attention models and previous select blocks models. Best results are in **bold**.

TREC 2023 Deep Learning Track Document Reranking		
Model	NDCG@10	MAP
Baseline models		
BM25	0.295	0.105
KeyB(BERT) _{BM25}	0.352	0.123
KeyB(BERT) _{BinB}	0.364	0.128
LLM		
RankLLaMA	0.386	0.133
RankLLaMA-MaxP	0.341	0.112
RankLLaMA-AvgP	0.349	0.117
KeyB2 models		
KeyB2(Llama2) _{BM25}	0.398 ^B	0.136
KeyB2(Llama2) _{cross}	0.421^{RB†}	0.143^{RB†}
KeyB2(Llama2) _{bi}	0.411 ^{RB}	0.141 ^{RB}
KeyB2(Llama3) _{BM25}	0.403 ^B	0.134
KeyB2(Llama3) _{cross}	0.412 ^B	0.138 ^B
KeyB2(Llama3) _{bi}	0.414 ^{RB}	0.139 ^B

Table 6. Results on *Robust04*. Left block: zero-shot transfer; right block: fine-tuned. Best scores in each block are **bold**.

Model	Zero-shot					Fine-tuned				
	P@10	P@20	MAP	NDCG@10	NDCG@20	P@10	P@20	MAP	NDCG@10	NDCG@20
Baseline models										
BM25	0.438	0.363	0.233	0.449	0.424	0.438	0.363	0.233	0.449	0.424
KeyB(BERT) _{BM25}	0.437	0.372	0.223	0.446	0.426	0.489	0.416	0.247	0.504	0.481
KeyB(BERT) _{BinB}	0.470	0.396	0.244	0.485	0.461	0.501	0.423	0.256	0.516	0.490
LLM										
RankLLaMA	0.459	0.386	0.229	0.474	0.450	0.468	0.405	0.230	0.476	0.457
RankLLaMA-MaxP	0.426	0.357	0.212	0.436	0.412	0.455	0.384	0.226	0.475	0.447
RankLLaMA-AvgP	0.416	0.362	0.212	0.427	0.413	0.446	0.380	0.223	0.462	0.440
KeyB2 models										
KeyB2(Llama2) _{BM25}	0.488 ^{R*‡}	0.407 ^R	0.240 ^R	0.498 ^R	0.471 ^R	0.527 ^{R‡}	0.445 ^{RB}	0.267 ^{R‡}	0.542 ^{R‡}	0.514 ^{RB}
KeyB2(Llama2) _{cross}	0.474	0.402 ^R	0.241 ^R	0.493 ^R	0.469 ^R	0.502 ^R	0.433 ^R	0.255 ^R	0.520 ^R	0.499 ^R
KeyB2(Llama2) _{bi}	0.472	0.399 ^R	0.238 ^R	0.490 ^R	0.466 ^R	0.535 ^{RB‡}	0.448 ^{RB‡}	0.269 ^{RB‡}	0.546 ^{RB‡}	0.517 ^{RB‡}
KeyB2(Llama3) _{BM25}	0.489 ^R	0.413 ^{RB}	0.247 ^{R†}	0.501 ^R	0.476 ^R	0.564 ^{RB}	0.475 ^{RB}	0.282 ^{RB}	0.576 ^{RB}	0.547 ^{RB}
KeyB2(Llama3) _{cross}	0.500^{RB*}	0.419^{RB*}	0.252^{R†*}	0.516^{RB†*}	0.489^{RB†*}	0.581^{RB}	0.480^{RB}	0.292^{RB†}	0.598^{RB†*}	0.559^{RB}
KeyB2(Llama3) _{bi}	0.478 ^R	0.407 ^R	0.244 ^R	0.490	0.469 ^R	0.567 ^{RB}	0.476 ^{RB}	0.288 ^{RB}	0.575 ^{RB}	0.546 ^{RB}

/ 0.288), this is a +4.1 % increase in NDCG@10 and +4.9 % in MAP, achieved with only 512 input tokens instead of 4096. All three selectors with Llama3 exceed both RankLLaMA (including MaxP, AvgP) and the previous best KeyB(BERT)_{BinB}.

- TREC DL23: On the MS MARCO v2 corpus (Table 5), KeyB2(Llama2)_{cross} yields 0.421 NDCG@10 and 0.143 MAP, corresponding to +9.1 % and +7.5 % over RankLLaMA (0.386 / 0.133). Every selector with

Table 7. Results on MLDR Chinese dataset. Best results are in **bold**.

Model	P@1	MAP	NDCG@8
Baseline models			
BM25	0.201	0.259	0.277
BERT based models			
KeyB(BERT) _{BM25}	0.423	0.586	0.685
KeyB(BERT) _{BinB}	0.804 ^R	0.876 ^R	0.907 ^R
LLM			
RankLLaMA	0.649	0.755	0.814
RankLLaMA-MaxP	0.374	0.554	0.661
RankLLaMA-AvgP	0.228	0.433	0.567
KeyB2 models			
KeyB2(Llama2) _{BM25}	0.864 ^{RB}	0.910 ^{RB}	0.932 ^{RB}
KeyB2(Llama2) _{cross}	0.929 ^{RB†}	0.955 ^{RB†}	0.966 ^{RB†}
KeyB2(Llama2) _{bi}	0.948 ^{RB†‡}	0.966 ^{RB†‡}	0.974 ^{RB†‡}
KeyB2(Llama3) _{BM25}	0.909 ^{RB}	0.942 ^{RB}	0.956 ^{RB}
KeyB2(Llama3) _{cross}	0.945 ^{RB†}	0.966 ^{RB†}	0.975 ^{RB†}
KeyB2(Llama3) _{bi}	0.946 ^{RB†}	0.965 ^{RB†}	0.974 ^{RB†}

Llama2 beats RankLLaMA (including MaxP, AvgP) and KeyB(BERT), confirming robustness under corpus shift.

- Robust04 (Zero-shot): When models trained on DL19 are evaluated on Robust04 without tuning (Table 6), KeyB2(Llama3)_{cross} achieves 0.516 NDCG@10 and 0.252 MAP. Relative to RankLLaMA (0.474 / 0.229), the gains are +8.9 % NDCG@10 and +10.0 % MAP. Even the BM25 selector surpasses all pooling baselines (RankLLaMA-MaxP / AvgP).
- Robust04 (Fine-tuned): After five-fold in-domain fine-tuning (Table 6), KeyB2(Llama3)_{cross} reaches 0.598 NDCG@10 and 0.292 MAP. This is +15.9 % and +14.1 % relative to the best non-LLM baseline KeyB(BERT)_{BinB} (0.516 / 0.256), and +25.6 % NDCG@10 score over the RankLLaMA score.
- MLDR-zh: On the Chinese long-document benchmark (Table 7), KeyB2(Llama2)_{bi} attains 0.948 P@1, 0.966 MAP, and 0.974 NDCG@8. Against RankLLaMA (0.649 / 0.755 / 0.814) this corresponds to +46.1 % P@1, +27.9 % MAP, and +19.7 % NDCG@8. All KeyB2 variants dramatically outperform both LLM (including the MaxP and AvgP models) and KeyB baselines, showing that the framework generalises beyond English corpora.

Across all five evaluation settings, KeyB2 consistently yields sizeable relative improvements over the strongest prior methods, irrespective of language or domain shift. The following subsections (6.2, 6.3 and 6.4) analyse these numbers in depth, addressing RQ2 (effectiveness), RQ4 (efficiency), and RQ3 (selector trade-offs), respectively.

6.2 Cross-Dataset Effectiveness Summary (Answer to RQ2)

Table 8 collates—for each collection—the strongest KeyB2 configuration and the two baselines of RQ2: full-document RankLLaMA and previous best block pre-ranking approach KeyB(BERT)_{BinB}. We report NDCG@10 or NDCG@8 as the main metric, together with relative improvements and significance markers from the detailed result tables.

Table 8. Best KeyB2 variant vs. RankLLaMA and KeyB(BERT)_{BinB}. Gains are relative (%).

Dataset	Metric	RankLLaMA	KeyB(BERT) _{BinB}	KeyB2 (best)
DL19	NDCG@10	0.701	0.697	0.731^{R,B} (+4.3 / +4.9)
DL23	NDCG@10	0.386	0.364	0.421^{R,B} (+9.1 / +15.7)
Robust04 (ZS)	NDCG@10	0.474	0.485	0.516^{R,B} (+8.9 / +6.4)
Robust04 (FT)	NDCG@10	0.476	0.516	0.598^{R,B} (+25.4 / +15.9)
MLDR-zh	NDCG@8	0.814	0.907	0.975^{R,B} (+19.8 / +7.5)

Key observations:

- Significant wins on every corpus: The winning KeyB2 variant is statistically superior to both baselines on all five evaluation settings, as indicated by the double superscript ^{R,B}.
- Magnitude of improvement: Gains over RankLLaMA span from +4.3 % (DL19) to +25.4 % (Robust04). Relative to KeyB(BERT)_{BinB}, improvements range from +4.9 % to +15.9 % on English corpora and +7.5 % on Chinese.
- Successful design: Comparing with RankLLaMA-MaxP and AvgP, the score pooling models, which perform relatively poor, the proposed select-then-combine-then-rerank design strategy of KeyB2 shows large improvements.
- Generalisation: Without in-domain tuning, KeyB2 still delivers significant gains on Robust04 (+8.9% NDCG@10); after fine-tuning the advantage widens to +25.4%.
- Language robustness: The framework remains highly effective on MLDR-zh where documents average over 12k tokens, confirming that KeyB2 is not limited to English data.

Conclusion for RQ2: Across five diverse evaluation settings, and with statistical significance in every case, KeyB2 which pairs an LLM reranker with an explicit block selector consistently outperforms both the full-document LLM baseline RankLLaMA (including MaxP, AvgP) and the strongest BERT-based block-selection system KeyB(BERT)_{BinB}, establishing the successful design (select-then-combine-then-rerank) of KeyB2, as a clearly more effective strategy for long-document ranking.

6.3 Efficiency and Resource Consumption

We compare the reranking time and GPU memory requirements of different models, as shown in Fig. 8. Each experiment is measured on a server with a NVIDIA A100 40GB GPU, Intel Xeon 6248R CPU, and 128GB memory, using the TREC 2019 DL document reranking dataset. Fig. 8a shows the average reranking time for 100 documents per query (note that the bi-encoder version precomputes block embeddings offline for fast online search). Fig. 8b records the GPU memory usage during efficient LoRA fine-tuning without gradient checkpointing with batch size 1. This setup demonstrates the minimum GPU requirements for training without advanced techniques like DeepSpeed ZeRO [41, 42] or gradient checkpointing, which may require multiple GPUs or reduce training efficiency.

6.3.1 Inference Time Comparison. The full-document RankLLaMA model requires 50.65 seconds to rerank 100 documents, making it the slowest approach due to autoregressive decoding over long inputs. In contrast, KeyB2 models significantly reduce inference latency by pre-selecting relevant blocks:

- KeyB2(Llama2)_{bi}: 6.25 seconds (87.7% faster than RankLLaMA)
- KeyB2(Llama3)_{cross}: 8.58 seconds (83.1% faster)
- KeyB2-BM25 variants: <6 seconds (fastest, over 88% faster)

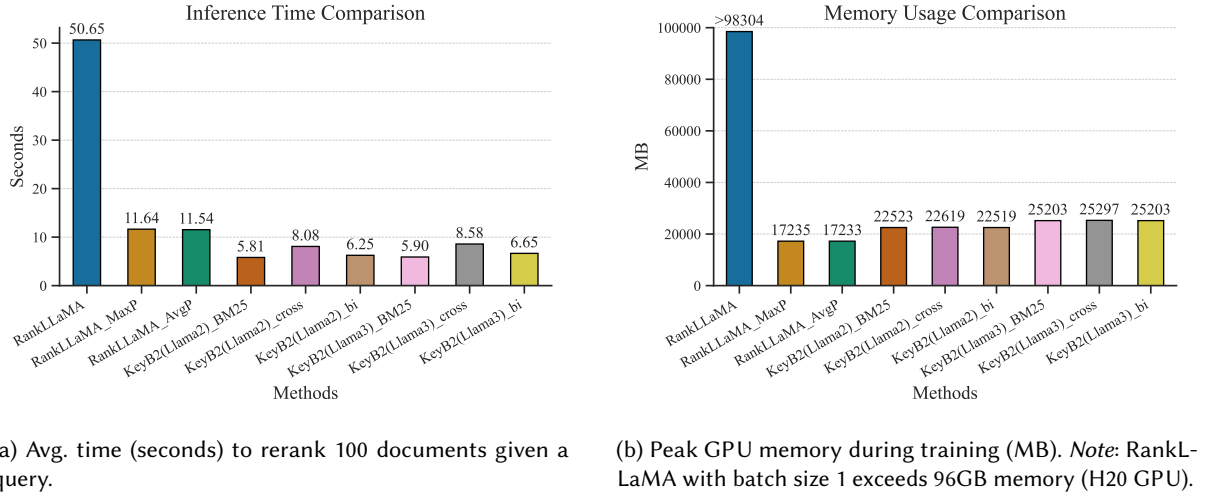


Fig. 8. Efficiency comparisons on TREC 2019 DL.

For comparison, RankLLaMA-MaxP (11.6 seconds) and AvgP (11.5 seconds), which average over segmented blocks, offer moderate efficiency improvements than RankLLaMA but remain around 35% slower than the slowest KeyB2 variant. These results highlight that block selection reduces inference time more effectively than post-hoc score aggregation.

6.3.2 Memory Requirements. Running RankLLaMA on full 4096-token documents requires over 96GB of GPU memory even with batch size 1, making training infeasible on standard GPUs without aggressive techniques such as gradient checkpointing, which introduce substantial overhead.

KeyB2 models drastically reduce memory demands:

- KeyB2(Llama2)_{BM25}: 22,523 MB (over 77% reduction vs. RankLLaMA)
- KeyB2(Llama3)_{cross}: 25,297 MB (over 74% reduction vs. RankLLaMA)

RankLLaMA-MaxP and AvgP are the most memory-efficient (17,235 MB), but as shown in Section 6.1, this comes at the cost of notable performance drops. KeyB2 models, by contrast, retain high accuracy while fitting comfortably on widely available hardware (e.g., NVIDIA 4090 for Llama2, V100/5090 for Llama3).

6.3.3 Pareto Frontier. Figure 9 plots NDCG@10 against latency and memory. All KeyB2 variants form or dominate the Pareto frontier in terms of speed: BM25 sits at the extreme efficiency corner, the bi-encoder offers the best quality-cost trade-off on the 7B backbone, and the cross-encoder pushes effectiveness to the maximum on 8B with acceptable overhead.

Conclusion for RQ4: Block selection drastically reduces computational overhead relative to full-document LLM reranker, RankLLaMA:

- 83–88 % lower inference latency (50.7 → 6–9 s per 100 docs).
- 74–77 % lower GPU memory during standard LoRA fine-tuning (> 96 GB → 22–25 GB)¹⁴.

¹⁴Without gradient checkpointing, which would slow training considerably.

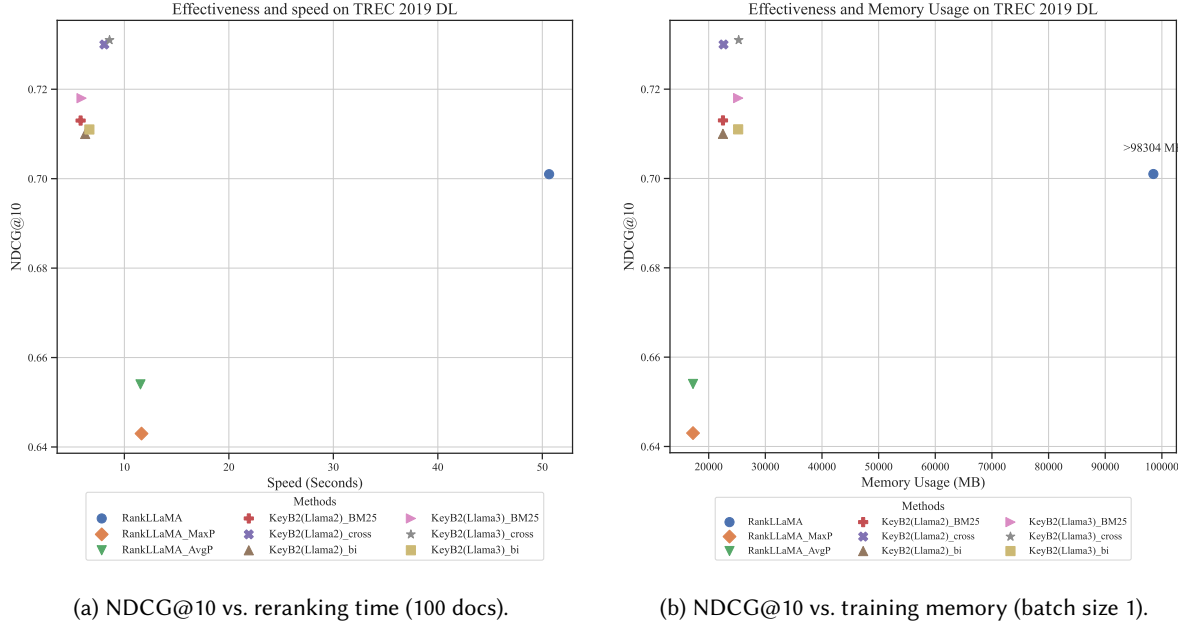


Fig. 9. Accuracy-efficiency trade-off on TREC 2019 DL (top-left is optimal).

Compared to RankLLaMA, which lies far outside the Pareto frontier, all KeyB2 variants offer superior accuracy-efficiency trade-offs. They consistently reduce computational cost while improving ranking effectiveness, thereby establishing a new Pareto frontier for LLM-based long-document reranking on a single 24–32 GB GPU.

Here we give an explanation about the above efficiency results. Although recent LLMs can handle input sizes from thousands to hundreds of thousands of tokens, their computational complexity still depends on the input token count. Similar to the Transformer or BERT architectures, recent LLMs like Llama2 or Llama3 also use self-attention mechanism. The difference is recent LLMs use the decoder-only architecture with unidirectional attention. Llama models use Grouped Query Attention (GQA) [1]: instead of each attention head having its own key (K) and value (V) matrices, multiple heads are grouped together, and each group shares the same key and value vectors. This mechanism is designed to reduce memory and computational overhead, particularly in large models like Llama and Mistral [20], by allowing several query heads to reuse the same key-value pair within a group. This helps speed up inference while maintaining the benefits of multi-head attention. Recent LLMs also use KV Cache [40] to speed up inference, but the KV Cache still faces memory bound issue. Besides, the cache does not apply to RankLLaMA. Indeed, the KV Cache technique caches the Key (K) and Value (V) matrices from previous tokens, enabling the model to reuse these stored results when generating new tokens. This avoids redundant computations and significantly improves efficiency. However, the RankLLaMA model only uses the last token to infer the relevance once and does not need to generate more tokens. Based on the above analyses, the complexity of the RankLLaMA model remains quadratic relative to the input token count. On the contrary, KeyB2 models use additional small models to filter out many irrelevant tokens, resulting in quadratic efficiency improvement.

6.4 Selector Design and Effectiveness–Efficiency Trade-off (RQ3)

Combining the effectiveness tables (Section 6.1) with the efficiency profiles (Section 6.3) yields the observations:

- (1) On TREC DL datasets, the cross-encoder is the strongest selector. The cross-encoder selector overall outperforms both BM25 and the bi-encoder on the TREC DL19 and TREC DL23 datasets. Specifically, on TREC DL19, KeyB2(Llama3)_{cross} significantly outperforms KeyB2(Llama3)_{bm25}, while KeyB2(Llama3)_{bi} shows no significant difference from BM25. On TREC DL23, KeyB2(Llama2)_{cross} also performs better and is significantly better than KeyB2(Llama2)_{BM25}, whereas KeyB2(Llama2)_{bi} is not. In addition, across datasets, the cross-encoder variant demonstrates the highest performance potential and peak results (e.g., on TREC DL and Robust04). This improvement comes at the cost of approximately 29.3% to 45.0% increased latency and only around 90 MB additional memory usage than other selectors.
- (2) On the Robust04 dataset, BM25 can be relatively strong. Under the zero-shot and Llama2 setting, KeyB2(Llama2)_{BM25} achieves the best performance, and KeyB2(Llama3)_{BM25} performs better than KeyB2(Llama3)_{bi}. Under the fine-tuned setting, KeyB2(Llama2)_{BM25} performs better than KeyB2(Llama2)_{cross}, and KeyB2(Llama3)_{BM25} performs similarly to KeyB2(Llama3)_{bi}. This may be because Robust04 documents average just over 700 tokens in length (see Table 2). As a result, the benefit of sophisticated learned selectors is limited. Block-level selection plays a less critical role, and BM25’s lexical signals may suffice to identify relevant content. This highlights a scenario where BM25-based selection remains competitive, especially when document length is moderate.
- (3) On the MLDR-zh dataset, bi-encoders generally perform better. KeyB2(Llama2)_{bi} shows significant improvements over both KeyB2(Llama2)_{bm25} and KeyB2(Llama2)_{cross}. KeyB2(Llama3)_{bi} performs similarly to the cross-encoder one, and both are significantly better than KeyB2(Llama3)_{BM25}. This indicates that bi-encoders can be particularly effective in certain settings, especially when the model is well-trained on the target language or domain, and can already capture sufficient semantic relevance. In such cases, the advantage of cross-encoders may not manifest, highlighting the importance of language and domain alignment in selector performance.
- (4) Efficiency and deployment trade-offs among selectors. In terms of inference efficiency, BM25 is the fastest and most lightweight option. It requires no model parameters or preprocessing, can be computed directly online using inverted indexes, and integrates seamlessly with KeyB2’s pipeline. Bi-encoder selectors offer a good balance between effectiveness and latency. Once block embeddings are pre-computed, online selection becomes fast and memory-efficient. However, this approach introduces engineering complexity and storage overhead due to the need for maintaining an external embedding index. Cross-encoders, while achieving the best accuracy on most English datasets, incur the highest runtime cost. They require scoring each block on-the-fly with the LLM, resulting in approximately 39–45% longer latency than BM25. Nevertheless, they are plug-and-play, requiring no offline indexing or embedding preparation, and incur only minimal memory overhead (around 90 MB compared to bi-encoder or BM25).

Answer to RQ3: Selector Design. Given the observations, we find that no single block selector dominates universally; instead, each offers a different balance of accuracy, efficiency, and engineering cost.

Cross-encoder deliver the highest accuracy across most English benchmarks, such as TREC DL19 and DL23, and achieve the strongest performance peak overall. It excels when document length exceeds (e.g., DL19 ~1.9k tokens) and token-level relevance modeling is needed. However, this comes at the cost of 29%–45% additional latency than bi-encoder and BM25, requiring real-time scoring of all blocks.

Bi-encoder offers a competitive alternative when the model is pretrained with strong alignment, as shown in MLDR-zh. It is more efficient once block embeddings are precomputed, but demand additional storage and

indexing efforts. Its effectiveness varies across tasks—while strong on MLDR-zh, it shows less consistent gains on TREC DL or Robust04.

BM25 remains a surprisingly strong baseline under certain conditions. On short documents (e.g., Robust04, ~700 tokens), where block selection is less critical, BM25 performs comparably or even better than learned selectors. It requires no training or offline computation and is the most deployment-friendly choice, particularly for latency-sensitive systems.

Overall, the block selector in KeyB2 serves as a tunable component to navigate the accuracy–efficiency spectrum:

- Use a cross-encoder when accuracy is the top priority and infrastructure supports modest latency increase.
- Use a bi-encoder when seeking a balance of speed and effectiveness, particularly when it is good enough under some settings.
- Use BM25 for maximum efficiency and simplicity.

These findings reinforce that selector design should be co-tuned with the LLM’s capacity, selector’s capacity, document length, and deployment constraints. KeyB2 enables flexible adaptation to such needs without compromising overall ranking quality.

6.5 Analysis of the Position of Selected Blocks

We analyze the block selection patterns across different strategies (BM25, cross-encoder, and bi-encoder) and datasets, as shown in Fig. 10. These figures show the probability distributions of the top 8 selected blocks across various document positions, highlighting trends in how different methods prioritize blocks within long documents.

6.5.1 Dataset-Specific Observations.

- TREC DL19 (MS MARCO) (Fig. 10a): All three methods show similar preferences for blocks in the front half. The cross-encoder focuses more on the front half, while the BM25 approach continues to emphasize the later positions, particularly the last three.
- TREC DL23 (MS MARCO v2) (Fig. 10b): Similar patterns are observed as in DL19, where all three methods predominantly select blocks from the first half. Compared to MS MARCO v1, MS MARCO v2 shows an even stronger concentration of selection in the early blocks, suggesting that relevant information in MS MARCO v2 tends to appear earlier within documents, while later blocks likely contain more non-relevant or noisy content.
- Robust04 (Fig. 10c): While early positions are still preferred, middle and later parts contribute more, particularly with the cross-encoder and bi-encoder methods. These strategies show a more distributed selection, retrieving relevant information from various positions and displaying a more spread-out pattern compared to TREC DL19.
- MLDR-zh (Fig. 10d): All three methods exhibit a stronger focus on early positions, with fewer blocks selected from later parts. This trend suggests that, for this Chinese dataset, relevant information may be more concentrated in the front positions. However, relevant information is still found and used in other positions, also contributing large portions.

6.5.2 *General Trends.* Across all datasets, over half of the top 8 selected blocks come from the first 5 positions in documents, reflecting a common positional bias where initial content is often more relevant to the query. These shows irrelevant noise tokens may be usually after the relevant tokens for these datasets. From Section 3.3, **we have shown inserting noise around the relevant document can result in poorer performance. On the contrary, our proposed approach can make the document contexts relevant-focused, with less noise information surrounding**, which would improve the attention weights and alignment (e.g., ARAS metric in

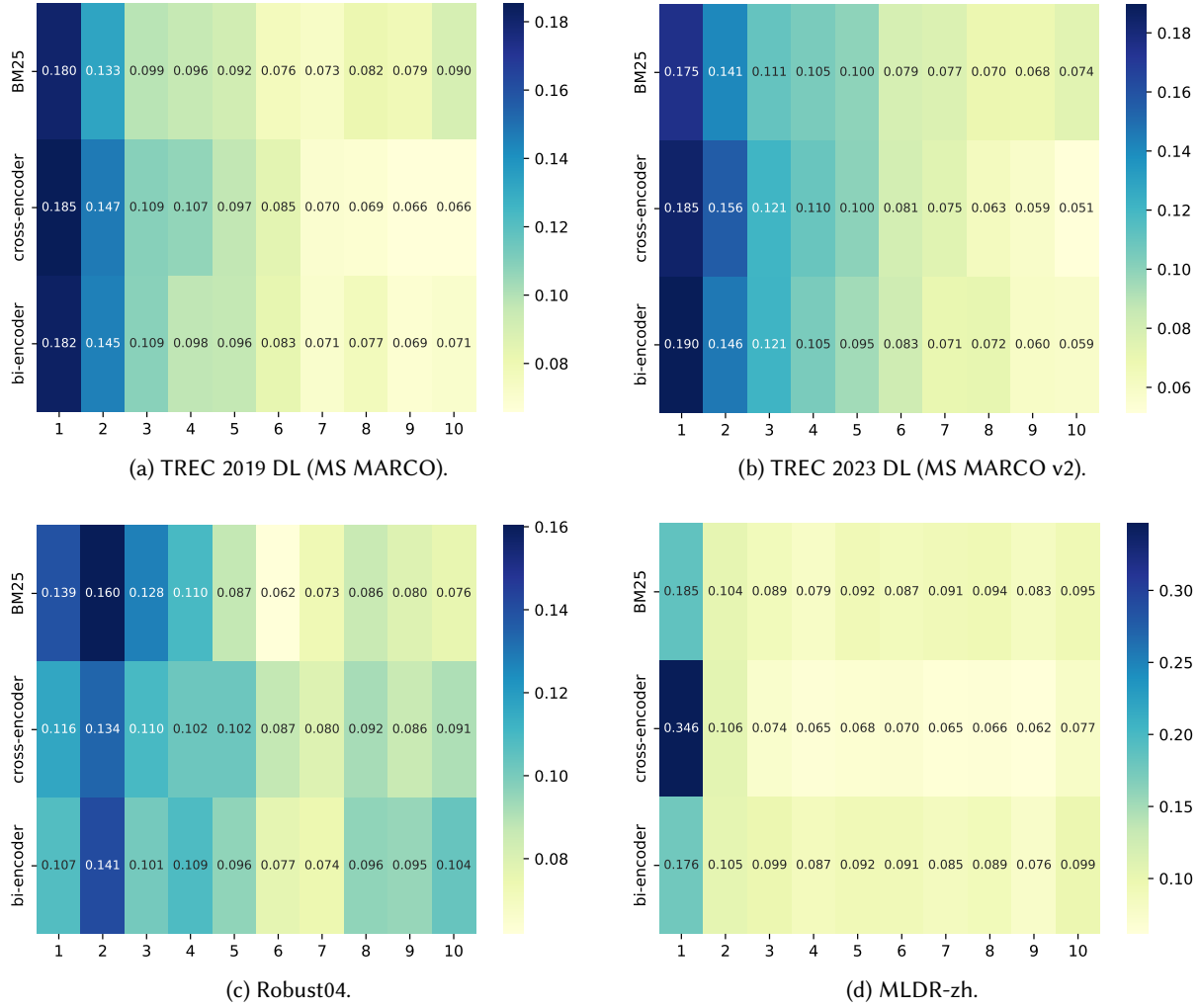


Fig. 10. The probabilities of top-8 block appearing locations across different datasets with various block selecting methods.

Section 3), and improve ranking performance. Additionally, the figures indicate that relevance distributions vary across datasets. While early positions dominate block selection across datasets, middle and later positions also contribute, indicating that the block selection approaches can retrieve relevant information from throughout the document when necessary.

7 Conclusion

We introduced **KeyB2**, a long-document retrieval framework that first selects salient blocks and then reranks them using decoder-only LLMs. Our attention analysis (**RQ1**) reveals that when irrelevant tokens are appended, especially near the end of a document, autoregressive LLMs exhibit severe attention dispersion, which undermines

relevance estimation. This finding motivates the design of an explicit select-then-combine-then-rerank pipeline with LLMs: KeyB2.

KeyB2 extends the original KeyB paradigm in three ways. First, based on the above analysis and findings from LLM-based IR models, we observe that even LLMs capable of processing longer sequences than BERT still suffer from noise, which hinders attention alignment between relevant parts and the query. This motivates the design of KeyB2. Second, it introduces a next-token-prediction-based scoring mechanism that is compatible with modern decoder-only LLMs. Third, it supports three families of block selectors (BM25, bi-encoder, and cross-encoder), with detailed experimental comparisons, allowing practitioners to trade off between accuracy and efficiency.

Experiments on TREC DL 2019/2023, Robust04, and MLDR-zh demonstrate consistent improvements over RankLLaMA, RankLLaMA-MaxP/AvgP, and earlier KeyB variants. KeyB2 achieves new SOTA results on TREC DL 2019 document reranking (**RQ2**). The cross-encoder selector achieves the highest scores on English benchmarks, while the bi-encoder variant performs best in MLDR-zh settings. The BM25 selector also performs well on Robust04, which contains documents of moderate length. These results suggest that the choice of selector should be co-tuned with the LLM’s capacity, the selector’s complexity, document length, and deployment constraints (**RQ3**). Analysis of the selected blocks shows that KeyB2 can surface relevant evidence regardless of its position within the document. This aligns with the findings in Section 3: less noise leads to stronger attention weights and better alignment (e.g., higher ARAS scores) compared to noisy contexts. Moreover, efficiency studies (**RQ4**) place KeyB2 on the Pareto frontier: it reduces inference time by up to 88% and peak GPU memory usage by over 74% compared to full-document RankLLaMA, while still improving effectiveness.

In short, even in the era of LLMs, selecting key blocks remains a critical component for effective long document ranking. By combining lightweight, explainable selectors with powerful decoder-only LLMs, KeyB2 provides a scalable and adaptable framework that not only enhances ranking performance, efficiency, but also inspires future advances in hybrid long document retrieval paradigms.

References

- [1] Joshua Ainslie, James Lee-Thorp, Michiel de Jong, Yury Zemlyanskiy, Federico Lebron, and Sumit Sanghai. 2023. GQA: Training Generalized Multi-Query Transformer Models from Multi-Head Checkpoints. In *Proceedings of the 2023 Conference on Empirical Methods in Natural Language Processing*. 4895–4901.
- [2] Iz Beltagy, Matthew E. Peters, and Arman Cohan. 2020. Longformer: The Long-Document Transformer. *arXiv:2004.05150*
- [3] Jianyu Chen, Shitao Xiao, Peitian Zhang, Kun Luo, Defu Lian, and Zheng Liu. 2024. M3-Embedding: Multi-Linguality, Multi-Functionality, Multi-Granularity Text Embeddings Through Self-Knowledge Distillation. In *Findings of the Association for Computational Linguistics ACL 2024*. 2318–2335.
- [4] Rewon Child, Scott Gray, Alec Radford, and Ilya Sutskever. 2019. Generating Long Sequences with Sparse Transformers. *CoRR abs/1904.10509* (2019).
- [5] Kevin Clark, Urvashi Khandelwal, Omer Levy, and Christopher D Manning. 2019. What Does BERT Look at? An Analysis of BERT’s Attention. In *Proceedings of the 2019 ACL Workshop BlackboxNLP: Analyzing and Interpreting Neural Networks for NLP*. 276–286.
- [6] Nick Craswell, Bhaskar Mitra, Emine Yilmaz, Daniel Campos, and Ellen M Voorhees. 2020. Overview of the TREC 2019 deep learning track. *arXiv preprint arXiv:2003.07820* (2020).
- [7] Zhuyun Dai and Jamie Callan. 2019. Deeper text understanding for IR with contextual neural language modeling. In *Proceedings of the 42nd International ACM SIGIR Conference on Research and Development in Information Retrieval*. 985–988.
- [8] Zihang Dai, Zhilin Yang, Yiming Yang, Jaime Carbonell, Quoc Le, and Ruslan Salakhutdinov. 2019. Transformer-XL: Attentive Language Models beyond a Fixed-Length Context. In *Proceedings of the 57th Annual Meeting of the Association for Computational Linguistics*.
- [9] Jacob Devlin, Ming-Wei Chang, Kenton Lee, and Kristina Toutanova. 2019. BERT: Pre-training of Deep Bidirectional Transformers for Language Understanding. In *Proceedings of the 2019 Conference of the North American Chapter of the Association for Computational Linguistics: Human Language Technologies, Volume 1 (Long and Short Papers)*, Jill Burstein, Christy Doran, and Thamar Solorio (Eds.). Association for Computational Linguistics, Minneapolis, Minnesota, 4171–4186. <https://doi.org/10.18653/v1/N19-1423>
- [10] Ming Ding, Chang Zhou, Hongxia Yang, and Jie Tang. 2020. Coglx: Applying bert to long texts. *Advances in Neural Information Processing Systems* 33 (2020), 12792–12804.
- [11] Scott Gray, Alec Radford, and Diederik P Kingma. 2017. Gpu kernels for block-sparse weights. *arXiv preprint arXiv:1711.09224* 3 (2017).

- [12] Jiafeng Guo, Yixing Fan, Qingyao Ai, and W Bruce Croft. 2016. A deep relevance matching model for ad-hoc retrieval. In *Proceedings of the 25th ACM international on conference on information and knowledge management*. 55–64.
- [13] Sebastian Hofstätter, Bhaskar Mitra, Hamed Zamani, Nick Craswell, and Allan Hanbury. 2021. Intra-Document Cascading: Learning to Select Passages for Neural Document Ranking. In *SIGIR '21: The 44th International ACM SIGIR Conference on Research and Development in Information Retrieval, Virtual Event, Canada, July 11-15, 2021*. 1349–1358.
- [14] Sebastian Hofstätter, Hamed Zamani, Bhaskar Mitra, Nick Craswell, and Allan Hanbury. 2020. Local self-attention over long text for efficient document retrieval. In *Proceedings of the 43rd International ACM SIGIR Conference on Research and Development in Information Retrieval*. 2021–2024.
- [15] Sebastian Hofstätter, Markus Zlabinger, and Allan Hanbury. 2020. Interpretable & Time-Budget-Constrained Contextualization for Re-Ranking. In *ECAI 2020 - 24th European Conference on Artificial Intelligence*, Vol. 325. IOS Press, 513–520.
- [16] Baotian Hu, Zhengdong Lu, Hang Li, and Qingcai Chen. 2014. Convolutional neural network architectures for matching natural language sentences. In *Advances in neural information processing systems*. 2042–2050.
- [17] Edward J Hu, Yelong Shen, Phillip Wallis, Zeyuan Allen-Zhu, Yuanzhi Li, Shean Wang, Lu Wang, and Weizhu Chen. 2021. Lora: Low-rank adaptation of large language models. *arXiv preprint arXiv:2106.09685* (2021).
- [18] Kai Hui, Andrew Yates, Klaus Berberich, and Gerard de Melo. 2017. PACRR: A Position-Aware Neural IR Model for Relevance Matching. In *Proceedings of the 2017 Conference on Empirical Methods in Natural Language Processing*. 1049–1058.
- [19] Kai Hui, Andrew Yates, Klaus Berberich, and Gerard De Melo. 2018. Co-PACRR: A context-aware neural IR model for ad-hoc retrieval. In *Proceedings of the eleventh ACM international conference on web search and data mining*. 279–287.
- [20] Albert Q Jiang, Alexandre Sablayrolles, Arthur Mensch, Chris Bamford, Devendra Singh Chaplot, Diego de las Casas, Florian Bressand, Gianna Lengyel, Guillaume Lample, Lucile Saulnier, et al. 2023. Mistral 7B. *arXiv preprint arXiv:2310.06825* (2023).
- [21] Jyun-Yu Jiang, Chenyan Xiong, Chia-Jung Lee, and Wei Wang. 2020. Long Document Ranking with Query-Directed Sparse Transformer. In *Proceedings of the 2020 Conference on Empirical Methods in Natural Language Processing: Findings*. 4594–4605.
- [22] Vladimir Karpukhin, Barlas Oğuz, Sewon Min, Patrick Lewis, Ledell Wu, Sergey Edunov, Danqi Chen, and Wen-tau Yih. 2020. Dense Passage Retrieval for Open-Domain Question Answering. In *Proceedings of the 2020 Conference on Empirical Methods in Natural Language Processing (EMNLP)*. 6769–6781.
- [23] Omar Khattab and Matei Zaharia. 2020. Colbert: Efficient and effective passage search via contextualized late interaction over bert. In *Proceedings of the 43rd International ACM SIGIR conference on research and development in Information Retrieval*. 39–48.
- [24] Nikita Kitaev, Lukasz Kaiser, and Anselm Levskaya. 2020. Reformer: The Efficient Transformer. *arXiv:2001.04451*
- [25] Alex Krizhevsky, Ilya Sutskever, and Geoffrey E Hinton. 2012. Imagenet classification with deep convolutional neural networks. *Advances in neural information processing systems* 25 (2012), 1097–1105.
- [26] Canjia Li, Andrew Yates, Sean MacAvaney, Ben He, and Yingfei Sun. 2020. PARADE: Passage representation aggregation for document reranking. *arXiv preprint arXiv:2008.09093* (2020).
- [27] Canjia Li, Andrew Yates, Sean MacAvaney, Ben He, and Yingfei Sun. 2023. PARADE: Passage Representation Aggregation for Document Reranking. *ACM Transactions on Information Systems* 42, 2 (2023), 1–26.
- [28] Minghan Li and Eric Gaussier. 2022. BERT-based dense intra-ranking and contextualized late interaction via multi-task learning for long document retrieval. In *Proceedings of the 45th International ACM SIGIR Conference on Research and Development in Information Retrieval*. 2347–2352.
- [29] Minghan Li and Eric Gaussier. 2024. Domain Adaptation for Dense Retrieval and Conversational Dense Retrieval through Self-Supervision by Meticulous Pseudo-Relevance Labeling. In *Proceedings of the 2024 Joint International Conference on Computational Linguistics, Language Resources and Evaluation (LREC-COLING 2024)*. 5247–5259.
- [30] Minghan Li, Diana Nicoleta Popa, Johan Chagnon, Yagmur Gizem Cinar, and Eric Gaussier. 2023. The power of selecting key blocks with local pre-ranking for long document information retrieval. *ACM Transactions on Information Systems* 41, 3 (2023), 1–35.
- [31] Percy Liang, Rishi Bommasani, Tony Lee, Dimitris Tsipras, Dilara Soylu, Michihiro Yasunaga, Yian Zhang, Deepak Narayanan, Yuhuai Wu, Ananya Kumar, et al. [n. d.]. Holistic Evaluation of Language Models. *Transactions on Machine Learning Research* ([n. d.]).
- [32] Qi Liu, Bo Wang, Nan Wang, and Jiaxin Mao. 2024. Leveraging passage embeddings for efficient listwise reranking with large language models. *arXiv preprint arXiv:2406.14848* (2024).
- [33] Yinhan Liu, Myle Ott, Naman Goyal, Jingfei Du, Mandar Joshi, Danqi Chen, Omer Levy, Mike Lewis, Luke Zettlemoyer, and Veselin Stoyanov. 2019. Roberta: A robustly optimized bert pretraining approach. *arXiv preprint arXiv:1907.11692* (2019).
- [34] Xueguang Ma, Liang Wang, Nan Yang, Furu Wei, and Jimmy Lin. 2024. Fine-tuning llama for multi-stage text retrieval. In *Proceedings of the 47th International ACM SIGIR Conference on Research and Development in Information Retrieval*. 2421–2425.
- [35] Rodrigo Nogueira and Kyunghyun Cho. 2019. Passage Re-ranking with BERT. *arXiv preprint arXiv:1901.04085* (2019).
- [36] Kezban Dilek Onal, Ye Zhang, Ismail Sengor Altingovde, Md Mustafizur Rahman, Pinar Karagoz, Alex Braylan, Brandon Dang, Heng-Lu Chang, Henna Kim, Quinten McNamara, et al. 2018. Neural information retrieval: At the end of the early years. *Information Retrieval Journal* 21, 2 (2018), 111–182.

[37] Hamid Palangi, Li Deng, Yelong Shen, Jianfeng Gao, Xiaodong He, Jianshu Chen, Xinying Song, and Rabab Ward. 2016. Deep sentence embedding using long short-term memory networks: Analysis and application to information retrieval. *IEEE/ACM Transactions on Audio, Speech, and Language Processing* 24, 4 (2016), 694–707.

[38] Liang Pang, Yanyan Lan, Jiafeng Guo, Jun Xu, Jingfang Xu, and Xueqi Cheng. 2017. DeepRank: A new deep architecture for relevance ranking in information retrieval. In *Proceedings of the 2017 ACM on Conference on Information and Knowledge Management*. 257–266.

[39] Fabian Pedregosa, Gaël Varoquaux, Alexandre Gramfort, Vincent Michel, Bertrand Thirion, Olivier Grisel, Mathieu Blondel, Peter Prettenhofer, Ron Weiss, Vincent Dubourg, et al. 2011. Scikit-learn: Machine learning in Python. *the Journal of machine Learning research* 12 (2011), 2825–2830.

[40] Reiner Pope, Sholto Douglas, Aakanksha Chowdhery, Jacob Devlin, James Bradbury, Jonathan Heek, Kefan Xiao, Shivani Agrawal, and Jeff Dean. 2023. Efficiently scaling transformer inference. *Proceedings of Machine Learning and Systems* 5 (2023), 606–624.

[41] Samyam Rajbhandari, Jeff Rasley, Olatunji Ruwase, and Yuxiong He. 2020. Zero: Memory optimizations toward training trillion parameter models. In *SC20: International Conference for High Performance Computing, Networking, Storage and Analysis*. IEEE, 1–16.

[42] Jeff Rasley, Samyam Rajbhandari, Olatunji Ruwase, and Yuxiong He. 2020. DeepSpeed: System optimizations enable training deep learning models with over 100 billion parameters. In *Proceedings of the 26th ACM SIGKDD International Conference on Knowledge Discovery & Data Mining*. 3505–3506.

[43] Nils Reimers and Iryna Gurevych. 2019. Sentence-BERT: Sentence Embeddings using Siamese BERT-Networks. In *Proceedings of the 2019 Conference on Empirical Methods in Natural Language Processing and the 9th International Joint Conference on Natural Language Processing (EMNLP-IJCNLP)*, Kentaro Inui, Jing Jiang, Vincent Ng, and Xiaojun Wan (Eds.). Association for Computational Linguistics, Hong Kong, China, 3982–3992. <https://doi.org/10.18653/v1/D19-1410>

[44] Devendra Sachan, Mike Lewis, Mandar Joshi, Armen Aghajanyan, Wen-tau Yih, Joelle Pineau, and Luke Zettlemoyer. 2022. Improving Passage Retrieval with Zero-Shot Question Generation. In *Proceedings of the 2022 Conference on Empirical Methods in Natural Language Processing*. 3781–3797.

[45] Keshav Santhanam, Omar Khattab, Christopher Potts, and Matei Zaharia. 2022. PLAID: an efficient engine for late interaction retrieval. In *Proceedings of the 31st ACM International Conference on Information & Knowledge Management*. 1747–1756.

[46] Keshav Santhanam, Omar Khattab, Jon Saad-Falcon, Christopher Potts, and Matei Zaharia. 2022. ColBERTv2: Effective and Efficient Retrieval via Lightweight Late Interaction. In *Proceedings of the 2022 Conference of the North American Chapter of the Association for Computational Linguistics: Human Language Technologies*. 3715–3734.

[47] Yelong Shen, Xiaodong He, Jianfeng Gao, Li Deng, and Grégoire Mesnil. 2014. A latent semantic model with convolutional-pooling structure for information retrieval. In *Proceedings of the 23rd ACM international conference on conference on information and knowledge management*. 101–110.

[48] Weiwei Sun, Lingyong Yan, Xinyu Ma, Shuaiqiang Wang, Pengjie Ren, Zhumin Chen, Dawei Yin, and Zhaochun Ren. 2023. Is ChatGPT Good at Search? Investigating Large Language Models as Re-Ranking Agents. In *Proceedings of the 2023 Conference on Empirical Methods in Natural Language Processing*. 14918–14937.

[49] Jesse Vig. 2019. A Multiscale Visualization of Attention in the Transformer Model. In *Proceedings of the 57th Annual Meeting of the Association for Computational Linguistics: System Demonstrations*. Association for Computational Linguistics, Florence, Italy, 37–42. <https://doi.org/10.18653/v1/P19-3007>

[50] Shengxian Wan, Yanyan Lan, Jun Xu, Jiafeng Guo, Liang Pang, and Xueqi Cheng. 2016. Match-SRNN: Modeling the Recursive Matching Structure with Spatial RNN. In *Proceedings of the Twenty-Fifth International Joint Conference on Artificial Intelligence, IJCAI*. 2922–2928.

[51] Chenyan Xiong, Zhuyun Dai, Jamie Callan, Zhiyuan Liu, and Russell Power. 2017. End-to-end neural ad-hoc ranking with kernel pooling. In *Proceedings of the 40th International ACM SIGIR conference on research and development in information retrieval*. 55–64.

[52] Lee Xiong, Chenyan Xiong, Ye Li, Kwok-Fung Tang, Jialin Liu, Paul N Bennett, Junaid Ahmed, and Arnold Overwijk. 2020. Approximate Nearest Neighbor Negative Contrastive Learning for Dense Text Retrieval. In *International Conference on Learning Representations*.

[53] Peilin Yang, Hui Fang, and Jimmy Lin. 2018. Anserini: Reproducible ranking baselines using Lucene. *Journal of Data and Information Quality (JDIQ)* 10, 4 (2018), 1–20.

[54] Sha Yuan, Hanyu Zhao, Zhengxiao Du, Ming Ding, Xiao Liu, Yukuo Cen, Xu Zou, Zhilin Yang, and Jie Tang. 2021. Wudaocorpora: A super large-scale chinese corpora for pre-training language models. *AI Open* 2 (2021), 65–68.

[55] Manzil Zaheer, Guru Guruganesh, Avinava Dubey, Joshua Ainslie, Chris Alberti, Santiago Ontanon, Philip Pham, Anirudh Ravula, Qifan Wang, Li Yang, and Amr Ahmed. 2021. Big Bird: Transformers for Longer Sequences. [arXiv:2007.14062](https://arxiv.org/abs/2007.14062)

[56] Longhui Zhang, Yanzhao Zhang, Dingkun Long, Pengjun Xie, Meishan Zhang, and Min Zhang. 2024. A Two-Stage Adaptation of Large Language Models for Text Ranking. In *Findings of the Association for Computational Linguistics ACL 2024*. 11880–11891.

[57] Chen Zhao, Chenyan Xiong, Corby Rosset, Xia Song, Paul Bennett, and Saurabh Tiwary. 2020. Transformer-XH: Multi-Evidence Reasoning with eXtra Hop Attention. In *International Conference on Learning Representations*.

[58] Kun Zhou, Yeyun Gong, Xiao Liu, Wayne Xin Zhao, Yelong Shen, Anlei Dong, Jingwen Lu, Rangan Majumder, Ji-rong Wen, and Nan Duan. 2022. SimANS: Simple Ambiguous Negatives Sampling for Dense Text Retrieval. In *Proceedings of the 2022 Conference on Empirical Methods in Natural Language Processing: Industry Track*. Association for Computational Linguistics, Abu Dhabi, UAE, 548–559.